DEVELOPMENT, THEORY, AND DESIGN OF THE IMAGE MOTOR FOR AUTOMOTIVE APPLICATIONS

A Thesis

Presented in Partial Fulfillment of the Requirements for the

Degree of Master of Science

with a

Major in Electrical Engineering

in the

College of Graduate Studies

University of Idaho

by:

Giselle S. Veach

July 2014

Major Professor: Herbert L. Hess, Ph.D.

Authorization to Submit Thesis

This thesis of Giselle Veach, submitted for the degree of Master of Science with a Major in Electrical Engineering and titled "Development, Theory, and Design of the Image Motor for Automotive Applications," has been reviewed in final form. Permission, as indicated by the signatures and dates below, is now granted to submit final copies to the College of Graduate Studies for approval.

Major Professor: _____ Date: _____

Herbert L. Hess, Ph.D.

Committee Members: _____ Date: _____

Brian K. Johnson, Ph.D.

_____ Date: _____

Dan Cordon, Ph.D.

Department Administrator: _____ Date: _____

Fred Barlow, Ph.D.

Discipline's College Dean: _____ Date: _____

Larry Stauffer, Ph.D.

Final Approval and Acceptance

Dean of the College of Graduate Studies: _____ Date: _____

Jie Chen, Ph.D.

Abstract

Current electric vehicles do not provide a reasonable range due in part to the inefficiencies and weight of the battery systems, the transmission, and the motors. To solve these problems some have suggested using a hub motor, however these motors are often heavy due to the selection of a DC or Synchronous machine. A better solution would be to use an adaptation of the linear induction motor. This thesis discusses the development of a theory based on image conductors that utilizes standard design techniques to design an image motor as well as the verification of this theory with Melcher's continuum mechanics. In addition this thesis discusses the process for designing such a machine as well as its optimal solution for an automotive application.

Acknowledgements

Dr. Hess's continuous support, guidance and constant encouragement have been invaluable in the development of this thesis. Without his assistance graduate school nor senior design would have been possible. Dr. Johnson graciously agreed to sit on my committee and his willingness to answer questions outside of class time helped develop an understanding of concepts used in this thesis. Dr. Law's machines course and passion for machines were an inspiration and without his help this thesis would have never been completed. Dr. Dan's willingness to help even when it was a little out of his expertise and he was willing to point in the direction of those who might know if he didn't. When I decided to pursue a second degree in electrical engineering, Dr. Egolf had faith in me and enabled me to get the second degree. Dr. Den Braven got me involved in research for the first time and helped me see my potential as a researcher. NIATT's gracious support allowed me to continue my education and develop the concepts in this thesis. And Tim Lenberg's assistance in development of the theories presented in this thesis was invaluable in understanding the concepts and developing the design and simulation tools.

Dedication

This thesis is dedicated to my family and friends who helped support me through my long education. My husband Tim stood by me through the ups and downs, listened to my crazy theories and withstood some of my hardest times. Without his assistance I would have never been able to develop any of the theories or models used in this thesis. My daughter Athena's smiles and laughter were sometimes all that got me through the day. My parents, Xiomi and Jerry supported me all these years and asked for nothing in return, without their support and help I would have never finished my degree. I thank all of them for all they do and have done throughout the years

Table of Contents

Table of Figures

Glossary

1 Background Information

1.1 Introduction

Electric vehicles (EV) have long been seen as the future of the automotive industry. With no direct emissions and no gasoline, many people have taken EVs to be the solution for those looking to live their lives in a more environmentally friendly manner, as well as people looking to end their dependence on foreign oil. For this reason, as soon as electric vehicles seemed viable, governments around the world instituted subsidies to encourage their development and sale. For example the United States created a subsidy in 2009 for a tax rebate of up to $7,500 for any purchase of an electric vehicle that met a basic set of criteria [1]. However, despite generous subsidies electric vehicles have failed to gain a significant portion of the automotive market, as electric vehicles make up only 0.62% of all automotive sales as of 2012 [2]. This lack of performance baffles many automakers and policy makers as they believe that the vehicles on the market meet the needs of the average consumer. They believe the average consumer's primary use of their vehicle is for their commute. In the United States many Americans commute around 50 miles in a day [3], so the automakers created vehicles to meet this demand which is evident by the vehicles in the $20-$40,000 price range having a distance per charge between 78 and 115 miles, an average round trip commute. So why are these vehicles not selling?

One possible explanation for lack of electric vehicle sales is travel. According to the American Travel Association 79% of all American leisure travel is done by automobile [4]. Some electric vehicle proponents would argue that in the average American two car household this is not an issue as they can have an electric vehicle for in-town driving and another gasoline vehicle for long distance travel. While in the past this would have been true, a recent New York Times article discussed a growing trend of Americans selling their second car to help make ends meet in these difficult economic times [5]. Still some may argue that with the gas savings that a family might see, they can afford to rent a car for their long-distance travel, but is that really viable?

As a thought experiment, consider a typical American family who travels three times a year; Christmas, Thanksgiving, and a one week vacation over the summer, and on average travels

250 miles each way on their vacations. This family has currently come onto the market for a new car and are considering purchasing an electric vehicle or a small sedan. They do some research and settle on the Ford Focus EV™ and the Mazda 3™ which are both within their price range. While the Focus will work fine for their daily driving, and will save them some money annually over the course of the year with an estimated operating cost of $618.00 a year [6], the Mazda 3™ can take them on their vacations although it has an operating cost of roughly $960.00 a year. The family considers both cars, and realizes that driving the Focus on their vacations is not an option as they would have to stop overnight at least 3 days due to the 78 mile range. They look into other electric cars and find that even the $68,000.00 Tesla with its 240 mile range falls short of their average distance. It is then decided that if they purchase the electric car they will rent a vehicle for their travel. The family then assumes one week per vacation and consults Enterprise-Rent-A-Car where they find that they can rent a car for $179.00 a week and as long as they stay within three states of their home state, they don't have to pay miles, although they do have to cover gas [7]. Assuming that gas will be the same for the Mazda or the rental, they do an analysis and find that when rental costs are factored in, the electric vehicle, with operating costs, will cost around $1555.00 a year to operate, so they purchase the Mazda.

Scenarios like the scenario above happen all the time in the U.S. where Americans weigh their options, and as evidence by USA Today's top 20 cars list, most Americans choose the gasoline vehicle [8]. Travel range, however, is not the only Achilles heel of electric vehicles. The average American family does not simply drive to and from work on a daily basis, a typical day for an American family can involve driving the kids to and from school, going grocery shopping, driving kids to after school activities, or any number of after work errands. With the range on an electric vehicle a family cannot feasibly run all their errands on a single charge and thus may not even consider the vehicle. As well, a recent top gear article referenced another problem with electric vehicles; the range is drastically impacted by electronics being turned on within the car. For example, air conditioning can take as much as 15 miles off of the range of the vehicle [9]. Given this, and that the interior of most cars can exceed 115 degrees in the summer without A/C, these cars are not safe to drive in areas where air conditioning in the car is a necessity.

Given that electric vehicles cannot make the range necessary for a long trip, cannot feasibly run an air conditioner without drastically effecting their range, and cannot realistically be used for long errands, it is clear that the number one problem facing electric vehicles is their range. The electric vehicle will not replace or compete with a gasoline vehicle which can make the range necessary for both daily driving and long trips. So how can the range problem be fixed?

1.2 Past Solutions

There are several ways that people have attempted to fix the problems with range. Research is currently being done in developing efficient regenerators, increasing the battery capacity, decreasing the weight, increasing the motor and transmission efficiency, and getting rid of the transmission entirely in favor of a direct drive solution. This section acts to help review a sampling of some of the existing technologies and ideas.

The first idea examined in this thesis is regenerative braking. During standard braking in a car, the brake calipers press down on the rotors causing the rotors and the attached wheel to come to a stop. This mechanical system converts the forward kinetic energy into considerable heat which is dissipated into the atmosphere. This heat becomes visible on a hot day, when the temperature of the surrounding air is too high to rapidly cool the brakes. On such a day, if the car is operating at over 100 mph or driving for a prolonged period on an incline where the brakes are applied to maintain speed, this heat becomes visible in the form of a considerable amount of smoke. Given the considerable energy lost in braking, a system which converts this energy back into a useful form could potentially extend the range of a vehicle.

A regenerative braking system does this. By utilizing a motor to stop the vehicle in lieu of or in addition to standard mechanical brakes, the energy from braking can be converted back to useful electrical energy, much like the heat recovery systems in a cogeneration or power plant. The effectiveness of this system depends on several things such as the placement of the motors, the type of motor used, and the method of regeneration.

An excellent regenerator will do as much of the overall braking with the motors as possible, and in an ideal regenerator the mechanical brakes will not be used at all. A typical regenerative braking system, such as that found on the world famous Toyota Prius, places the

regenerative braking system on the rear wheels while using mechanical brakes to make up for any braking not done by the regenerator [10]. The efficiency of such a system can recover much of the braking energy on the rear wheels, however such a design requires that all stops are done normally. It is important to note, however, that most of these systems do not operate in such a way as to recover all of the energy on the rear wheels and are designed with a regenerator and standard mechanical brakes. In the Toyota Prius^{TM}, for example, the efficiency of the mechanical brakes on the front and rear are advertised as a selling feature. This leads to the assumption that the braking system was designed for an optimal mechanical system which typically works such that 70-90% of braking is done on the front axle [11]. If this is the case, only 30% of all energy is available to the rear wheels, and such a regenerator will not be efficient. If regeneration is to be used, it is necessary to design for the regenerator to work as the brakes and to install mechanical brakes as a backup. If the regenerator is designed such that the braking is done on the rear, or such that there are regenerators on all four wheels it is theoretically possible to recover all of the braking energy. In actuality, however, a regenerator is incapable of recovering all of this energy. The amount of energy that can be recaptured is highly dependent on the type of motor chosen.

The two most commonly used motors in electric vehicles are the permanent magnet synchronous and permanent magnet Direct Current (DC) machines. In the past DC machines were unparalleled in their ease of use, control and speed range. With a fairly simple control, uniform torque could be obtained with a wide-range of speeds up to rated speed, and speed could be easily controlled with armature voltage alone with predictable and realizable dynamics that made them simple to analyze for design purposes. In the past when computation was difficult and mobile computation was rare it was difficult to generate with mobile AC machines, thus DC machines were preferred for generation. In contrast to the DC machines, as small motors synchronous machines are unparalleled in their torque per gram and torque per Amp. Without the cumbersome field winding, and no need for mechanical sensors, the permanent magnet synchronous depends solely on frequency for accuracy of speed. As a generator, the permanent magnet synchronous machine provided relatively good generation, relying only on speed for generation and if properly designed for a niche application they can be relatively "unbeatable". But here is where the automotive industry is

stuck in the past. A properly controlled induction machine can provide much better torque characteristics than a DC machine, and is much more rugged [12]. In addition, while the small permanent magnet synchronous machines provide amazing torque and require only speed to produce voltage, an induction machine can be considerably lighter. This is due to the fact that a properly controlled induction machine can produce the same torque while utilizing lighter weight aluminum for the rotor. So what is it about an induction machine that makes it more ideal? What is the behavior of an induction machine, and why is it, potentially, a better regenerator?

Unlike the synchronous and DC machines, the induction machine has a much better characteristic for regeneration. As can be seen in Figure 1-1, which depicts the general shape of an induction motor torque speed curve, the induction machine can produce more torque during generation than during motoring. This torque is ideal for braking, as the increased torque allows for shorter braking times and the less time to brake means that more of the braking can be done in the regenerator as opposed to via mechanical brakes. This means that more of the overall braking energy can be recovered in the regenerator. More recovered energy then directly translates to an increased range.

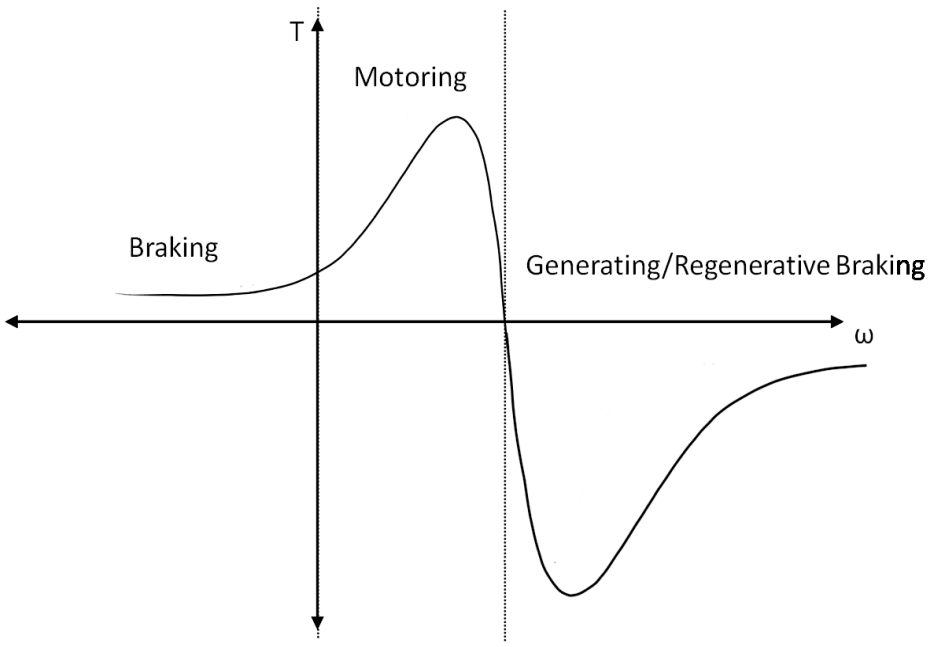

Figure 1-1 Induction Motor Torque Speed curve

Using an induction machine to regenerate can be done in one of two ways. Either the regeneration can be done in the braking region of the torque curve, in which case the machine will stop more abruptly and less energy will be recovered. This is due to the fact that high current will cause losses in the form of dissipated heat. These losses help the machine to stop more abruptly. Or, a control scheme known as Volts per Hertz can be used, so that the optimal negative torque position can be maintained as the vehicle decreases in speed. This process is generally slower than operating in the braking region, however a greater amount of energy can be recovered.

It is also necessary to note that regeneration will not significantly increase range during long trips as the brakes are going to be rarely used, thus very little energy will be recovered during trips. Regeneration, however, can be considerable in city driving and especially during the work day when traffic can require frequent stops. This means that a regenerator would be useful in extending the range for work-day driving and for errands around town. It also means that it is necessary to implement another solution in order to extend the range for long distance travel.

A common solution for the range issue is to add more batteries to the pack. In theory if the battery capacity, or the energy density of the batteries, can be increased then the range can be increased proportional to the available energy. Or in other words if the capacity of the battery pack is doubled the distance per charge can be doubled. While in theory this is true, the battery pack would have to maintain the same weight while doubling capacity. This doubled capacity for the same weight involves creating a battery with a better power density, and although currently research is being done to this end, in practice to double the capacity of the batteries the weight must also be doubled.

Take for example a Ford Focus EV, according to their website the car has a curb weight of roughly 3640 lbs. The battery pack makes up roughly 650 lbf of this weight [13]. As an example assume that the coefficient of rolling resistance between the tires and the road is 0.015, there are no losses, and the motor size does not have to be increased to compensate for weight. In addition estimate that the car sees roughly 360 N of drag force while traveling at 60

mph. This example will give the graph shown in Figure **1-2** which shows the increase in driving distance per increase in weight in per unit.

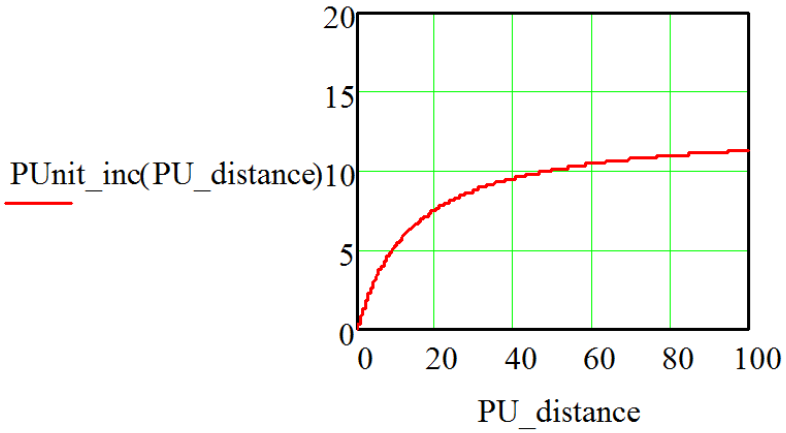

Figure 1-2: Per Unit increase in distance for percent increase in battery capacity

It is evident from the graph this is not a linear relationship. For example doubling the size of the Ford Focus EV™'s battery pack will only yield a 0.86 per unit increase in range, and only a 1.5 per unit increase in range for a pack that is triple the size. This happens because an increase in battery capacity yields a proportional increase in weight, and the increased weight leads to increased friction resistance. In addition the size of the battery packs may necessitate a re-design of the car chassis in order to accommodate the new batteries. This re-design could lead to more wind-resistance which will also lead to decreased distance, although this is not shown in the figure above. This wind resistance problem becomes more of an issue if the solution to increase range provided by many automobile manufacturers is used.

The solution provided by these automakers involves installing enough batteries inside the vehicle for a usual daily commute, and then installing a hitch to facilitate connection of a trailer to the vehicle for long distance travel [14]. If more distance is required, a higher capacity trailer or multiple trailers could be used. In other words, assuming that the vehicle has a 78 mile range, one trailer has "enough" energy for an additional 100 mile range, and a family needs to travel 240 miles, then the family can hitch two trailers to the car and drive the distance. This solution still poses two additional problems; the first being that there is a limit

to how many trailers a non-commercial vehicle can tow, and the second being that in addition to the weight issue discussed above there is now an even worse drag issue faced by the car. This means that what would appear to be 278 miles of travel distance would in fact be 185 miles when only weight is considered, and even less if the drag on the trailers is factored in. What this means is that there is an optimum number of useful batteries and past that point the added expense is not worth the small increase in distance achieved.

One of the biggest problems with modern electric vehicles is their weight. As was discussed above weight directly affects distance traveled. This can sometimes be compensated for by using more powerful motors, but still the added weight will drastically effect the distance that can be traveled. Take the difference between the gas mileage on a Mazda 3 and an SUV. An SUV will get considerably lower gas mileage despite its more powerful engine because of its weight. This leads into the idea of the power to weight ratio which is a metric that allows for direct comparison of the capabilities of two vehicles. A higher power to weight ratio means that more energy is available to propel the car. This is similar to a horse and cart, a single horse pulling an empty lightweight cart will be able to pull the cart faster and farther than the same horse pulling a heavy cart loaded down with bricks. This same comparison can be made between an electric vehicle and its gasoline counterpart. For example, the Ford Focus™ standard hatchback has an estimated starting weight of 2960 lbs with a 160 hp motor, where its electric counterpart has a weight of 3640 lbs and makes use of a 107 kW, approximately 143 hp, electric motor [13]. This means that the power to weight ratios for these two vehicles are 0.054 hp/lbf, and 0.039 hp/lbf respectively. This shows that the gasoline vehicle's performance is an improvement of 38.462 percent over the electric vehicle. So what does this say about how to improve electric vehicles?

The performance analysis above shows that weight is a large factor in the overall performance of an electric vehicle, and leads to a desire to decrease weight and/or increase power. There are several main sources of weight in a vehicle; the transmission, the motor, and the batteries. In order to decrease weight, these sources must be addressed. One method, discussed above, is to create batteries with a better power density. Another involves making a lighter weight electric motor. Perhaps the most promising way to decrease the weight is to eliminate the transmission by directly connecting the motors to the wheels. Weight by itself will not,

however, fix every shortcoming in the range, many of the shortcomings in the range come from the lack of efficiency in the drive system.

The most common solution to fix the drive system efficiency is to create a more efficient motor. By losing less energy in the motor, more of the energy provided by the batteries is being used for propulsion and less energy is then needed overall. The higher speed a motor is designed for, the easier it is to produce a better efficiency for a lower weight. It is fairly common knowledge that as speed is decreased weight of the machine must increase, or in order to obtain a lighter weight machine for a given speed, efficiency must be sacrificed. For this reason many manufacturers opt to use a higher speed motor so that they can obtain a higher efficiency. This poses another problem, though, as in order to utilize the higher speed motor a transmission must be used in order to bring the speed down for practical use.

A typical drive train is between 85 and 90% efficient depending on the drive train being rear wheel or front wheel drive [15]. This means that in a typical system the losses are between 10 and 15%. As losses are additive, losses in the motor will compound within the transmission leading to an even greater loss. For example, if a motor is 90% efficient, and the drive train is 85% efficient, the efficiency of the total system is only 76.5% efficient. Even if the motor is 99% efficient, the total efficiency will only be 84.6% efficient. This innate inefficiency means that without considering both the motor and the transmission in the design, no matter how efficient the motor is, losses in the mechanical system will always degrade overall system efficiency. In addition the larger the ratio required to gear the motor down to road speed will require a larger transmission and therefore reducing the improvements caused by decreasing the machine weight.

Due to the innate inefficiencies in the transmission and their weight, it has been suggested that the transmission be removed and the motors be direct connected to the wheels, either through placing the motors in the center of the vehicle and connecting them via a shaft to the wheels, or placing the motor on or in the wheel hub. Many of these solutions face either the problem of high inefficiencies or high weights. The most promising of these motors is the Protean Electric hub motor. This motor weighs roughly 68 lbs and has an efficiency of roughly 90% [16]. The problem with motors such as the Protean Electric is that they must be attached to a

standard wheel which is equivalent to adding a 68 lb weight to the wheel of a car. Other motor solutions involve hub motors that can exceed 350 lbs. Motor solutions such as this are problematic, as it is well known that unsprung mass on the wheels can pose problems with handling, ride and fatigue on the suspension. This means that in order to utilize a hub motor, the motor must be low weight. Many of these motors are permanent magnet synchronous, permanent magnet DC, or reluctance machines which are innately heavy. But what about the induction machine?

1.3 Proposed Solution

The induction machine has long been considered the work horse of industry. With their aluminum squirrel cage rotor and wound stator these machines are typically far more robust than their synchronous or DC counterparts and also typically boast a lighter weight. One variation on the squirrel cage induction motor is the flat plate linear induction machine. This motor consists of an aluminum rail and a flat stator that typically looks like a standard stator has been unrolled into a linear form. These linear motors have been used for over one hundred years for trains, steel manufacturing, and monorails as well as other applications. There is a direct advantage to these machines as they do not require as thick of a back iron as a squirrel cage machine, and can have a much thinner aluminum rotor. Instead of heavy permanent magnets or copper windings the rotor can be replaced with lightweight aluminum. In addition the use of multiple poles and a higher frequency on the stator would allow for a smaller and lighter weight stator while still maintaining the low speeds required for a direct drive. If one of these machines was adapted to an inside-out radial topology, the machine could theoretically fit within the standard size of a wheel. This means that such a machine could become the vehicle's wheel, eliminating the need for a wheel or for specialty supports. Such a motor would eliminate the need for a transmission and could theoretically be designed to fall within the 25-40 lbs typical of a standard wheel. This would mean that motors could be added to the vehicle without adding any extra weight. In fact this would effectively act to increase power to weight ratio and overall efficiency of the system.

1.4 Summary

Although electric vehicle technology is advancing, consumer sales have not followed. The most likely reason for this is the low range of commercially available electric vehicles.

Research is being done in several areas to try to improve the range, unfortunately these solutions have fallen short. A new solution would be the application of a linear induction motor to a direct drive solution. This allows for the creation of extremely light weight and relatively efficient motors without the use of a gearbox and therefore helps to improve power to weight ratio, efficiency and overall range. The theory to explain the operation of these motors will be presented in the following chapter.

1.5 References

[1] Tesla, "Electric Vehicle Incentives Around the World," *Tesla*, 2014. [Online]. Available: http://www.teslamotors.com/incentives/US. [Accessed: June 04,2014]

[2] J. Cobb, "December 2013 Dashboard," *hybridCARS*, 2014. [Online]. Available: http://www.hybridcars.com/december-2013-dashboard/. [Accessed: June 19, 2014]

[3] United States Census Bureau, "Megacommuters: 600,000 in U.S. Travel 90 Minutes and 50 Miles to Work, and 10.8 Million Travel an Hour Each Way, Census Bureau Reports," *United States Census Bureau*, 2014. [Online]. Available: http://www.census.gov/newsroom/releases/archives/american_community_survey_acs/cb13-41.html. [Accessed: June 10,2014]

[4] U.S. Travel Association, "Travel Facts and Statistics," *U.S. Travel Association*, 2014. [Online]. Available: http:// www.ustravel.org/news/press-kit/travel-facts-and-statistics. [Accessed: June 10, 2014]

[5] M. Noor, "Many Families Limiting Themselves to a Single Car," *The New York Times*, 2008. [Online]. Available: http://www.nytimes.com/2008/07/27/nyregion/nyregionspecial2/27Ronecar.html?ref=nyregionspecial2&_r=0. [Accessed: June 10, 2014]

[6] CPS Energy, "The Cost of Charging Your Electric Vehicle," *CPS Energy*, 2014. [Online]. Available: http://www.cpsenergy.com/About_CPS_Energy/Who_We_Are/Research_and_Technology/Plug_In_Vehicles/PlugIn_recharging_cost.asp. [Accessed: June 10, 2014]

[7] Enterprise Rent-A-Car, *Enterprise Rent-A-Car*, 2014. [Online]. Available: http://www.enterprise.com/car_rental/afterHours.do. [Accessed: June 14, 2014]

[8] C. Woodyard, "Gas prices rattle April's 20 top-selling cars list," *USA Today*, [Online] Available: http:// www.usatoday.com/story/money/cars/2014/05/02/best-selling-cars-april/8587507/. [Accessed: June 14, 2014]

[9] S. Philip, "First Drive: VW e-Golf," *TopGear,* 2014. [Online]. Available: http://www.topgear.com/uk/car-news/volkswagen-e-golf-first-drive-2014-03-21. [Accessed: June 14,2014]

[10] Toyota, "Features & Specs", *Toyota*, 2014. [Online]. Available: http://www.toyota.com/prius/features.html#!/mechanical_performance/1223/1225/1227/122. [Accessed: June 14,2014]

[11] J. Erjavek, *Automotive Brakes*, 1st ed. Clifton Park, NY; Thompson Delmar Learning, 2006. [E-Book]: Available: Google Books.

[12] H. Hess. "Fwd: Dc machines" Personal email (June 25, 2014)

[13] Ford, "FOCUS Specifications", *Ford*, 2014. [Online]. Available: http://www.ford.com/cars/focus/specifications/engine/ [Accessed: June 14, 2014]

[14] N. Gordon-Bloomfield, "Forget Better Place, Hook Your electric Car To a Battery Trailer", *Green Car Reports*,[Online] Available: http://www.greencarreports.com/news/1079294_forget-better-place-hook-your-electric-car-to-a-battery-trailer/ [Accessed: June 20, 2014].

[15] D.Cordon. "RE: Thesis Corrections" Personal email (Jul 16, 2014)

[16] Protean Electric, "Overview", *Protean Electric,* 2014. [Online] Available: http://www.proteanelectric.com/en/overview/ [Accessed: June 20, 2014]

2 Theory

The theory behind how force is generated in the linear induction motor is not generally understood. To this end many theories have been postulated by various universities to explain motion in a linear motor. In addition it is generally considered impossible to design a linear motor using standard design techniques due to a lack of understanding. Often a mix of finite element analysis and what will be called the "build and toss" method are used to design these machines. In this report, existing analysis techniques and theories with regard to the operation and design of these motors will first be discussed, then a theory based on image theory that is consistent with Melcher's analysis of tachometers will be presented [1].

2.1 Existing Analysis Techniques and Theories

A search of IEEE Xplore for linear induction motor design will produce a myriad of papers both claiming to have a functional lumped parameter model and that the only way to design one of these machines is through finite element analysis. There are two main papers that discuss a lumped parameter model, "The Analytical Calculation of the Thrust and Normal Force and Force Analyses for Linear Induction Motor" by Ghang, Quiang, Zhiming, Yi and Guo-guo [2], and "Research of the Performance Characteristics of Linear Induction Motor" by Xu, Sun, and Li [3]. It is impossible to provide a thorough analysis of the theories presented in these papers as both papers are lacking either in proof or available references. Reference [2] presents an in-depth theory which involves determining winding factors for the purpose of calculating inductances, however the lack of theoretical proof for their theories as well as the lack of numbers for verification of their experimental evidence renders this reference unusable. Reference [3], which discusses the idea that the linear motor can be analyzed the same as a rotary induction motor presents a theory which appears to match the experimental evidence presented, however use of their theory is dependent on a specific reference, this reference cannot be obtained in the United States as it was published in China with limited availability and even if it was obtained it is written in an uncommon dialect of Chinese which would be difficult and costly to have translated. Therefore it is impossible to replicate their results in the United States.

Aside from these two papers, most other papers require a finite element analysis of the machine. From a discussion with Dr. Jeffry Young, an electromagnetics expert with the University of Idaho, while finite element analysis by itself is a useful simulation tool in order to verify an existing design, it cannot, by itself, be used as a design tool unless a concrete theory is known, in which case that should be used in lieu of finite element analysis. The methodology of finite element analysis is as follows: first a finite element model must be used in order to get a better understanding of the theory, then the theory must be used to create a new finite element model. This methodology must be followed until a model appears to give a desired result, at which point the device must be built and tested. Once the device is built it must then be compared to the finite element model and a new model must be created if there is significant difference.

Finite element analysis leads to what will be called the "build and toss" method. This method involves using some theory to build a scale model of the desired machine. The scale model is then tested and analyzed for its behavior. If the model does not behave as desired it is thrown out and a new model is created. This is done for multiple rotors and stators until the desired performance is obtained. It is evident from the simple methodology that this method can become expensive fairly quickly as a single machine can be thousands of dollars to build. Finite element often gets into the build and toss method, bringing it down in cost some as some of the permutations are done on a computer. The problem with this is that there will still have to be several prototypes built before a desirable behavior is obtained.

Another problem with finite element analysis is its general incompatibility with other models. The best automotive designs integrate the mechanical and electrical design models and simulate dynamics as effected by both. This integrated analysis allows all components to be computer-tested before fabrication. In other words, an integrated computer model allows designers to "drive" the car without building a prototype. By doing this, all changes can be made on a computer before hardware is built, thus decreasing prototyping expenses and the number of prototypes that must be built. A finite element model cannot be easily integrated with other electrical and mechanical models, thus making them undesirable for systems in which an integrated model is necessary.

In order to create a worthwhile design methodology for one of these linear motors, the theory behind why they work must be developed. There have been many discussions as to why these machines develop force. Some theorize that end effects cause the force. Others theorize that the force is generated by the imbalance in charge on the rotor, or that it is the stator seeking a lower energy state in the rotor that induces force [4]. The problem with these theories is that they are either not supported by experiment, or they are difficult to align with a logical analysis. It is evident from the above that it is necessary to develop a worthwhile theory that can accurately describe the motion in a linear motor.

2.2 Development of a Theoretical Model Of the Linear Motor

When one looks in a mirror, one sees a reflection of oneself at the same distance from the mirror on the opposite side. The clarity of this image and the quality of replication of the original depends on the properties of the material which is used to create the mirror. This happens because when a light wave is incident on a reflective surface the wave will be both reflected and refracted. This behavior can be seen in Figure **2-1** below.

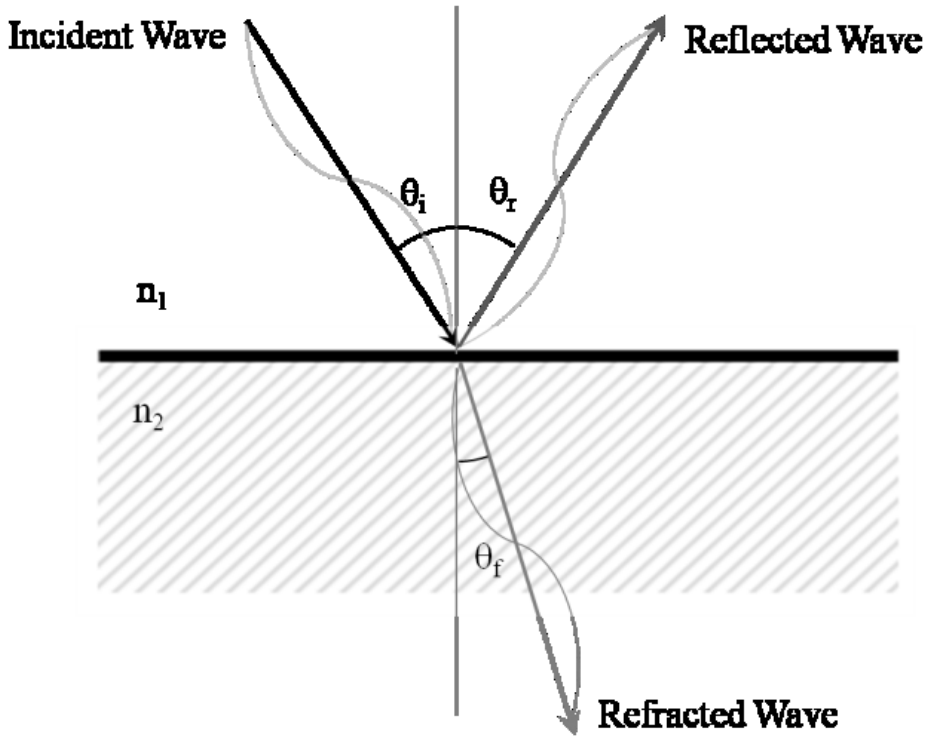

Figure 2-1: Reflection and Refraction of a Light Wave

The theory of optics tells us that an electromagnetic wave can be reflected and/or refracted by a medium depending on the material properties of that medium. Or in other words if a wave is incident to a medium by a given angle, θ_i, it will be reflected at the angle of reflection, θ_r, and refracted by a ratio of the material properties and the sine of the angle of incidence, or:

$$\frac{\sin(\theta_i)}{\sin(\theta_r)} = \frac{n_2}{n_1} \quad \text{(eq. 1)}$$

Where n is the index of refraction of each medium and the angles are given by (eq. 1). A perfect mirror will perfectly reflect the incident wave with no refraction. If instead of light, the light wave is replaced by the electromagnetic waves produced by a coil of wire, the mirror will be replaced by a conducting material. The electromagnetic wave will be reflected by the conducting material perfectly if the conducting material is a perfect conductor. Or in other words a reflection of the coil of wire will appear to be inside of the conducting material as shown in the figure below.

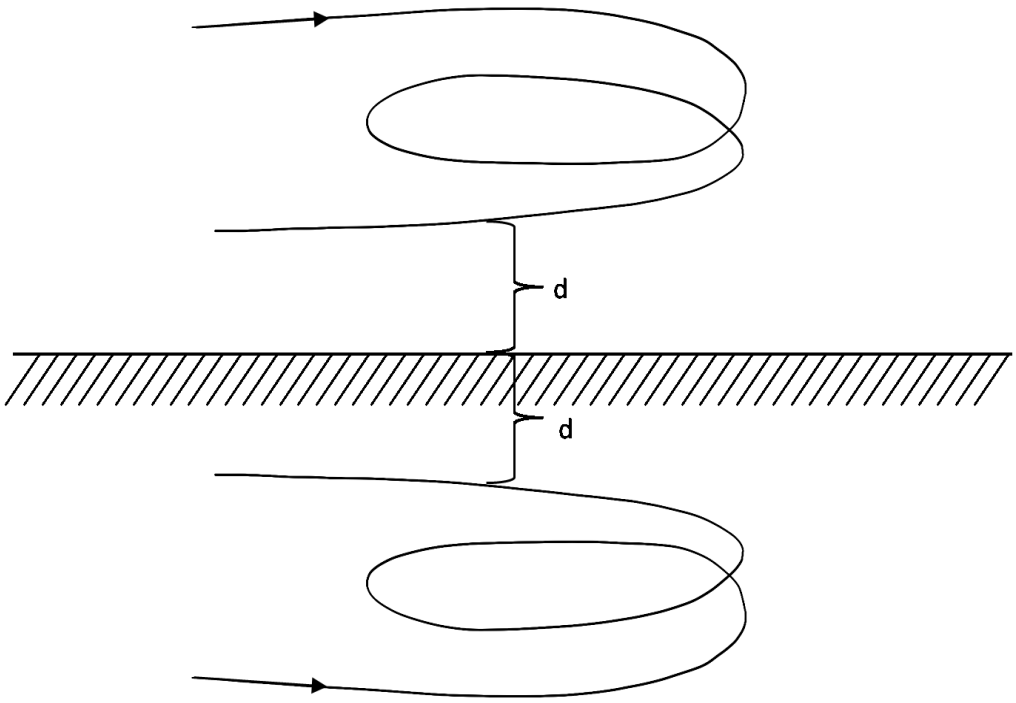

Figure 2-2: Reflection of a Coil of Wire

This reflection will have the same resistance of the coil of wire, so long as the conductor is a perfect conductor. If the conductor is imperfect, the resistance of the coil of wire will be

proportional to the difference in conductivity between the coil and conducting materials. Or in other words it will be as shown in (eq. 2) where the subscript, r, refers to the reflection, c, refers to the coil, and cs refers to the conducting surface.

$$R_r = \frac{\mu_{cs}}{\mu_c} R_c \qquad \text{(eq. 2)}$$

If an iron core is then placed within the coil and a magnetically permeable material is placed behind the conducting medium, then the inductance seen by the coil will be the same as the inductance seen by the reflection and the mutual inductance of the coil and its reflection will be the same as if the conducting surface and permeable material were replaced by an identical coil and core. In other words the magnetic field will have a return path through the magnetic material and the behavior of the fields will be such that there appears to be two coils and cores although there is only one. So what happens when there are multiple coils?

There is an experiment in physics in which the light is turned out in the room, a slit is cut in a sheet of paper and placed a distance from a wall. A flashlight is then shined on the sheet of paper and what is known as a diffraction or interference pattern appears on the wall. This experiment is shown in Figure 2-3 below.

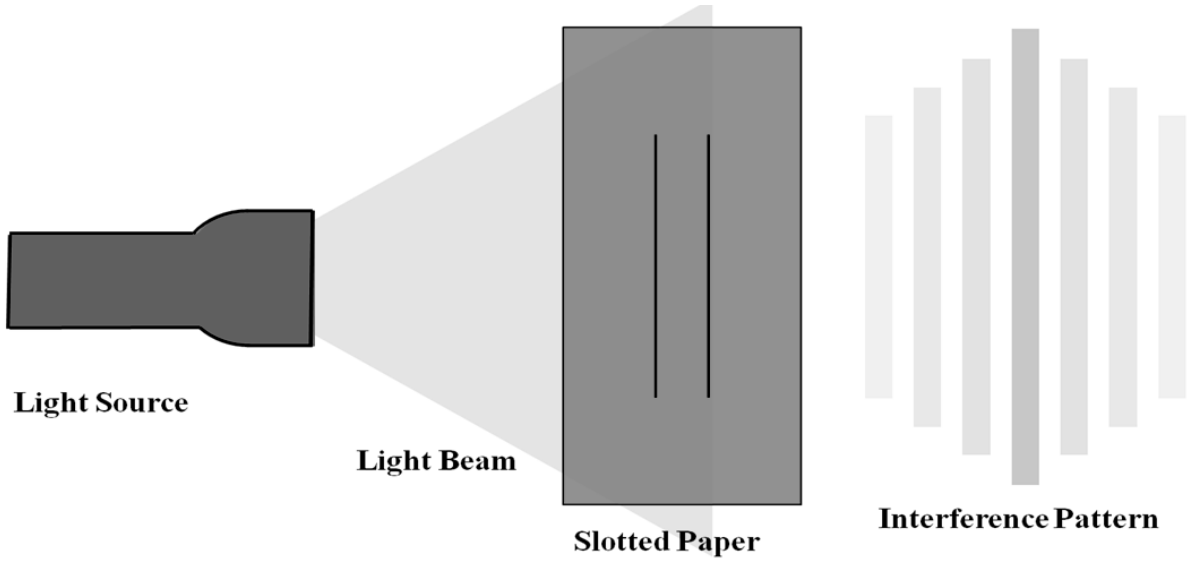

Figure 2-3: Light Diffraction Experiment

In this experiment the interference happens because of the phase shift of the light as it goes through the slots in the paper. The waves are at different phases relative to one another and thus interference happens. This can be visualized in the case of a wave:

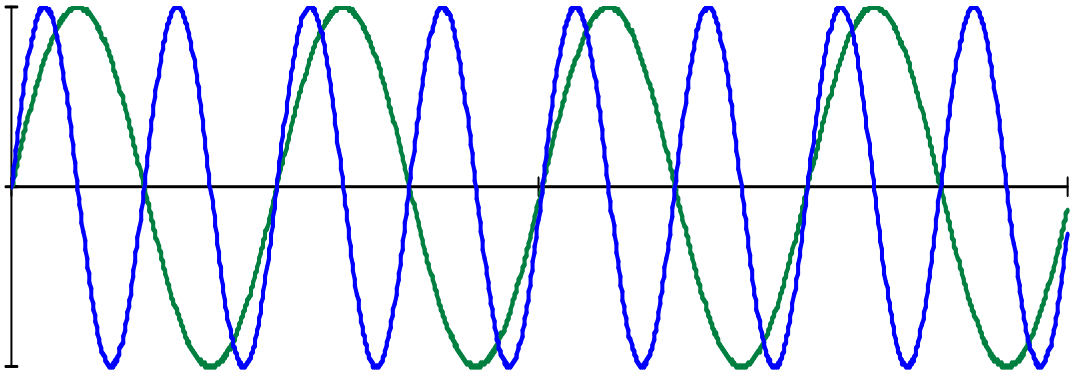

Figure 2-4: Interfering waves

Figure 2-4 shows a sketch of two waves of differing frequencies. If these two waves are added the graph in Figure 2-5 is obtained.

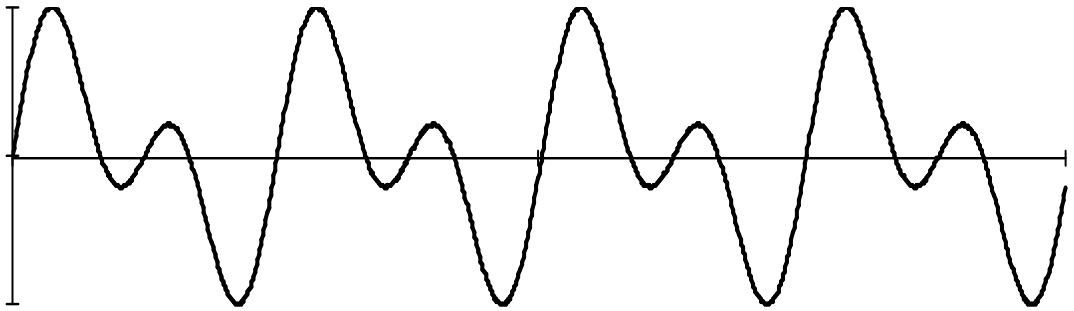

Figure 2-5: Addition of waves

As is evident from 2-5 the waves will interfere constructively in some places and interfere destructively in others leading to larger peaks in some places and smaller peaks in others. This same interference pattern happens when multiple coils are placed over a conducting surface and will lead to a non-uniform magnetomotive force (mmf). The nonuniformity of this mmf will lead to motion as high energy fields seek a lower energy state within the media, thus inducing motion. Just as a more intense wave can be obtained by increasing the intensity of

the light beam, either by using a more powerful bulb or increasing the number of bulbs (see an LED flashlight), a stronger magnetic field and thus an increased force can be obtained by using multiple coils.

This then introduces the driving theory behind how to design an inside out linear induction motor. Given that the conducting plate is reasonably thin, the stator which is nothing more than multiple wound coils, will be reflected by the conducting plate and thus produce interference and force on the rotor. As long as the rotor material is adhered such that the material will not be affected by the increased force, the interference in the magnetic fields of the stator and rotor will produce a force and thus motion on the rotor. In other words, the rotor will be a direct reflection of the stator provided that the difference in conducting materials is taken into account.

In chapter 4 of Melcher's Continuum Mechanics [1] he discusses the development of the parameters for a smooth stator machine. In his discussion of the machine he assumes surface currents for the stator given as:

$$K_z^s = \mathrm{Re}[|I_a|e^{j\omega t}N_a \cos(ky) + |I_b|e^{j\omega t}N_b \cos(k\left(y - \frac{\ell}{4}\right))] \qquad \text{(eq. 3)}$$

Where the parameters are given from the following figure:

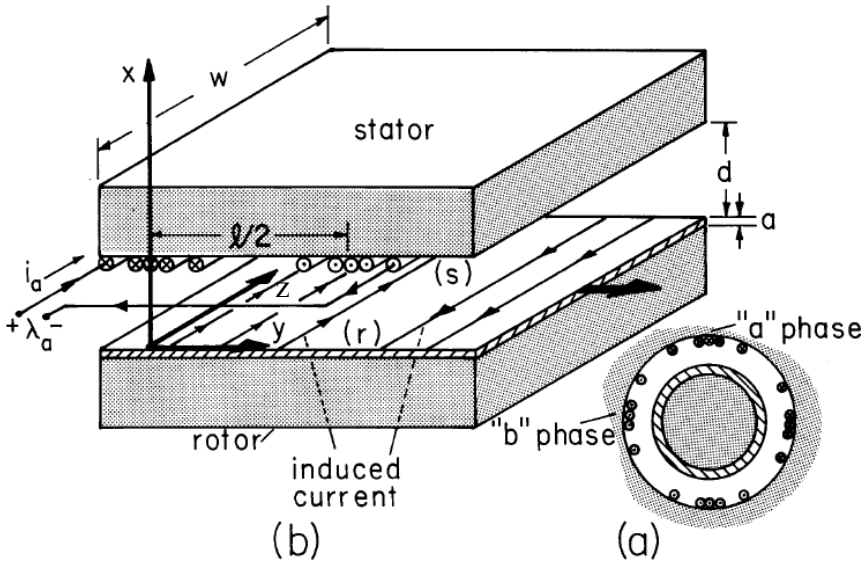

Figure 2-6: Figure 6.4.1 in Melcher's Continuum Mechanics [1]

Melcher defines ℓ as twice the axial length of one coil, N_a and N_b are the number of turns in the a and b phases respectively, ω is the electrical frequency in the coil, and I_a and I_b are defined as the phasor representations of the a and b currents. And where k is defined as:

$$k = \frac{2\pi}{\ell} \quad \text{(eq. 4)}$$

In which ℓ is defined as the same as above. By using Euler's formula (eq. 3) can be written as:

$$K_z^s = \mathrm{Re}[\hat{K}_+^s e^{j(\omega t - ky)} + \hat{K}_-^s e^{j(\omega t + ky)}] \quad \text{(eq. 5)}$$

Where

$$\hat{K}_\pm^s = \frac{1}{2}(|I_a|N_a + |I_b|N_b e^{\pm\frac{jk\ell}{4}}) \quad \text{(eq. 6)}$$

This writes the excitation in terms of a complex amplitude Fourier series. In this case of Melcher's tachometer there are only two main terms, which correspond to waves propagating in the positive and negative z directions. Because the equations satisfy linear bulk and boundary equations, the response to (eq. 5) is the superposition of the positive and negative terms.

It is convenient to define the air gap fields in terms of vector potentials because the flux linkages need to be computed. This means that $\hat{B}_x = -jk\hat{A}$. If the rotor and stator materials are assumed to be "infinitely permeable", boundary conditions on the stator and rotor will follow from Ampere's law and the boundary condition of the stator will be:

$$\hat{H}_y^s = -\hat{K}_s \quad \text{(eq. 7)}$$

The composite boundary condition for the thin sheet is give as:

$$\hat{H}_y^r = \frac{\sigma_s}{k}(\omega - kU)(-jk\hat{A}^r) \quad \text{(eq. 8)}$$

The fields due to the stator and rotor are then related by:

$$\begin{bmatrix}\hat{A}^s \\ \hat{A}^r\end{bmatrix} = \frac{\mu_0}{k}\begin{bmatrix}-\coth(kd) & \frac{1}{\sinh(kd)} \\ \frac{-1}{\sinh(kd)} & \coth(kd)\end{bmatrix}\begin{bmatrix}\hat{H}_y^s \\ \hat{H}_y^r\end{bmatrix} \quad \text{(eq. 9)}$$

Combining the last three equations, then, to find the rotor surface current which is given by $\hat{H}_y^r$ with ampere's law, the following is obtained:

$$\hat{H}^{r}_{y\pm} = -\frac{\hat{K}^{s}_{\pm} S_{m\pm}[j+S_{m\pm}\coth(kd)]}{\sinh(kd)[1+{S_{m\pm}}^{2}\coth(kd)^{2}]} \quad \text{(eq. 10)}$$

Where the dimensionless number S_m combines the ratio of a magnetic diffusion time, the characteristic time, and the magnetic Reynolds number so that:

$$S_{m\pm} = \frac{\mu_0 \sigma_s}{k}(\omega \mp kU) \quad \text{(eq. 11)}$$

In order to compute the voltages necessary to deliver the currents I_a and I_b, the flux linkages must be found. These flux linkages are found from:

$$\Phi_\lambda = w\left[\hat{A}^{s}(y') - \hat{A}^{s}\left(y' + \frac{\ell}{2}\right)\right] \quad \text{(eq. 12)}$$

If this is written as the superposition of the two field components, this becomes:

$$\Phi_\lambda = w\,\mathrm{Re}\left[2(\hat{A}^{s}_{+}e^{-jky'} + \hat{A}^{s}_{-}e^{jky'})e^{j\omega t}\right] \quad \text{(eq. 13)}$$

In the interval of dy', where y=y', there are $N_a \cos(ky')\,dy'$ turns, and thus the flux linked by the a phase is given by:

$$\lambda_a = \int_{-\ell/4}^{\ell/4} \Phi_\lambda(y') N_a \cos(ky')dy' = wN_a\mathrm{Re}\left[\int_{-\ell/4}^{\ell/4}\left(\hat{A}^{s}_{+}e^{-jky'} + \hat{A}^{s}_{-}e^{jky'}\right)\left(e^{jky'} + \right.\right. \quad \text{(eq. 14)}$$

$$\left.\left. ejky'ej\omega tdy'\right.\right.$$

Only the constant terms will contribute to the integration, therefore after integrating and substituting the flux becomes:

$$\lambda_a = \frac{w\ell}{2}\frac{N_a}{k}\mu_0\mathrm{Re}\left[\coth(kd)\left(\hat{K}^{s}_{+} + \hat{K}^{s}_{-}\right) + \frac{\hat{H}^{r}_{y+} + \hat{H}^{r}_{y-}}{\sinh(kd)}\right]e^{j\omega t} \quad \text{(eq. 15)}$$

This same line of reasoning can be used to calculate the flux in b, and from the above calculations the equations for inductance and resistance can be calculated:

$$L_1 = L_2 = \frac{wN_a{}^2\ell^2\mu_0}{4\pi}\tanh\left(\frac{\pi d}{\ell}\right) \quad \text{(eq. 16)}$$

$$M = \frac{wN_a{}^2\ell^2\mu_0}{4\pi\sinh\left(\frac{2\pi d}{\ell}\right)} \quad \text{(eq. 17)}$$

$$R = \frac{\ell w N_a{}^2}{2\sigma_s} \quad \text{(eq. 18)}$$

In these equations N_a is given as turns per unit length, and σ_s is given by:

$$\sigma_s = a\sigma \quad \text{(eq. 19)}$$

Where a, as given in Figure 2-6, is the thickness of the conducting plate, and σ is the conductivity of the conducting material. In these equations R is simply the rotor resistance, as the stator resistance is considered negligible, and Melcher's leakage terms assume an ideal stator without discrete slots, this lack of discrete slots means that the only leakage term has to do with air gap fringing, and thus the leakage terms will be much smaller than the leakage in the true machine. Melcher's model does show that the leakage terms will be reflected and the rotor resistance will be referenced from the stator windings which illustrates the abovementioned theory.

In the following chapter the development of the lumped parameter model used for design will be discussed, and the final design parameters will be given showing how the calculations from the final design model align with Melcher's formulations.

2.3 Summary

There have been many theories postulated as to how the linear induction motor operates, and from these theories different design methodologies have been developed. These design methodologies range from lumped parameter models to utilizing finite element analysis and prototyping to design a viable machine. These design methodologies each have their own problems, however, as many of the papers which present lumped parameter design methods are difficult to verify, and a finite element model, while being more expensive, cannot be easily used for further simulation of the whole system. It is clear that a new theory must be developed to further define how these machines function. From the method of images a theory is developed that is consistent with a continuum mechanics analysis as performed by Melcher.

2.4 References

[1] Melcher, James R. *Continuum Electromechanics*. Cambridge, MA: MIT Press, 1981. Copyright Massachusetts Institute of Technology. ISBN: 9780262131650. Also available online from MIT OpenCourseWare at http://ocw.mit.edu (Accessed June 21,2014) under Creative Commons license Attribution-NonCommercial-Share Alike.

[2] L.V. Ghang, LI Quiang, LIU Zhiming, FAN Yu and LI Guo-guo, "The Analytical Calculation of the Thrust and Normal Force and Force Analyses for Linear Induction

Motor", *Signal Processing, 2008. ICSP 2008. 9th International Conference,* 26-29 Oct. 2008 [Abstract] Available: IEEE Xplore, http://ieeexplore.ieee.org/ [Accessed: April 10, 2013]

[3] Wei Xu, Guangsheng Sun and Yaohua Li, "Research on Performance Characteristics of Linear Induction Motor", Industrial Electronics and Applications, 2007. ICIEA 2007. 2nd IEEE Conference*,* 23-25 May 2007 [Abstract] Available: IEEE Xplore, http://ieeexplore.ieee.org/ [Accessed: April 10, 2013]

[4] E.F. da Silva, E.B. dos Santos, P.C.M. Machado, M.A.A. Oliveira, "Dynamic Model for Linear Induction Motors", Industrial Technology, IEEE International Conference, 2003, [Abstract] Available: IEEE Xplore, http://ieeexplore.ieee.org/ [Accessed: April 10, 2013]

3 Development of the Lumped Parameter Model

It is important to have an accurate lumped parameter model which accounts for a realistic, non-ideal stator and its parameters as reflected to the rotor. As per the discussion in Chapter 2, standard design methods should be viable as long as it is recognized that the rotor parameters will simply be an inexact mirror of the stator parameters. The lumped parameter model was developed from theories presented by both Lipo in his Introduction to Machine Design [1], and Alger in The Induction Machine [2]. This section will begin with a discussion of resistance calculations, then it will discuss the magnetizing and leakage inductances and it will conclude with an analysis of calculated values and their comparison with the calculations derived by Melcher. The lumped parameter model used is shown in Figure 3-1:

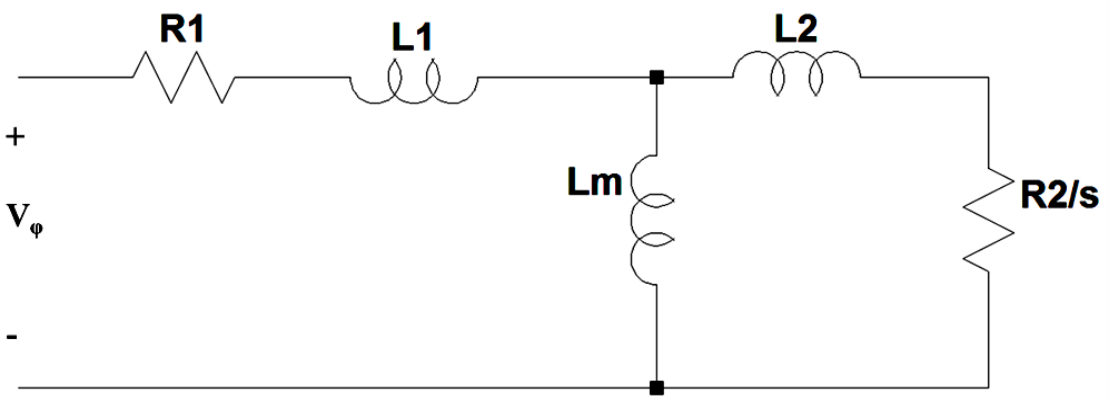

Figure 3-1: IIM lumped parameter model

3.1 Resistance Calculations

Previous to this chapter, this particular machine was called the inside out radial linear induction motor, however from this point forward this machine will be called the Image Induction Machine (IIM) due to the rotor being, essentially, the image of the stator. This is done, partially to shorten the name, and partially because once radial, this machine bears no further resemblance to the linear motor other than the flat plate rotor. The resistance calculations were derived after a discussion with Tim Lenberg, another graduate student in Electrical Engineering. It is to be noted that the important calculation here is the stator resistance, as the rotor resistance will simply be a reflection of the stator.

The stator resistance will be determined from the following basic equation:

$$R_s = \frac{(\text{Length of Coil})(\text{Number of Turns})(\text{Resistivity of Coil Material})}{(\text{cross sectional Area of single wire})} \quad \text{(eq. 20)}$$

In terms of variables:

$$R_s = \frac{4\mathfrak{L}_c N_s \rho_{stator}}{\pi {d_w}^2} \quad \text{(eq. 21)}$$

Where N_s is the number of series turns. The length of a single coil can be calculated from the following equation:

$$\mathfrak{L}_c = w + p\tau_p + d_w \quad \text{(eq. 22)}$$

where the terms are defined as follows:

$\mathfrak{L}_c$ = length of a coil
w = effective length of machine
p = pitch of a coil
τ_p = width of a slot pitch
d_w = diameter of a single wire

And where τ_p is calculated from:

$$\tau_p = n_s q \frac{\pi(D+g_1)}{N_{slots}} \quad \text{(eq. 23)}$$

with the terms defined as:

n_s = number of stator slots per phase belt
q = phase belts per pole
D = stator diameter
g_1 = air gap
N_{slots} = number of slots

And where the effective air gap and the stator diameter are calculated from:

$$D = (d - t_r)\frac{2PP}{2PP+0.1\pi} \quad \text{(eq. 24)}$$

$$g_1 = \frac{0.1\pi D}{2PP} \quad \text{(eq. 25)}$$

where the terms are defined as:

PP = pole pairs
d = outer diameter of the machine

t_r = thickness of rotor

The rotor resistance will be the reflection of the stator resistance accounting for the difference in conducting material between the rotor sheet and the stator windings.

$$R_r = \frac{\rho_{rotor}}{\rho_{stator}} R_s \quad \text{(eq. 26)}$$

This is similar to (eq. 2), however it uses resistivity terms. It is important to note that a the thicker the rotor plate, the lower the rotor resistance will be and the less valid the theory is. The rotor resistance and derivation above and for Melcher's work is assuming a reasonably thin rotor plate such that $ak \ll 1$.

3.2 Magnetizing Inductance

The magnetizing inductance refers to the mutual inductance between the rotor and the stator coils. Inductance of a coil refers to the number of flux linkages in Weber turns per Ampere of current flowing in a coil. This term, "Weber turns per Ampere" is defined as a Henry. The magnetizing inductance is made up of several pieces, and is most easily explained by presenting the equation itself and discussing its subsequent parts as they appear. The magnetizing inductance of a coil is given by:

$$M = \frac{3}{2}\left(\frac{N_{se}}{2PP}\right)^2 \mu_0 \pi \frac{rw}{g_2} \quad \text{(eq. 27)}$$

Where this equation is taken from reference [1]. And where the terms are defined as follows:

N_{se} = Number of equivalent series turns
μ_0 = permeability of free space ($4\pi 10^7$ H/m)
r = radius of stator
g_2 = effective air gap

The two terms that need to be defined, here, are the equivalent series turns and the effective air gap. The effective air gap is given by the following:

$$g_2 = k_c g_1 \quad \text{(eq. 28)}$$

Because the first part of this equation is given above, the term that must be defined is k_c. This term is called the Carter factor, and is defined such that.

$$k_c = k_{cs} k_{cr} \quad \text{(eq. 29)}$$

However, because the rotor is a direct mirror of the stator, this term is simply the square of the stator factor such that:

$$k_c = {k_{cs}}^2 \quad \text{(eq. 30)}$$

The carter factor is then calculated by:

$$k_{cs} = \frac{\tau_s}{\tau_s - \frac{2b_0}{\pi}\left\{\operatorname{atan}\frac{b_0}{2g_1} - \frac{g_1}{b_0}\ln\left[1+\left(\frac{b_0}{2g_1}\right)^2\right]\right\}} \quad \text{(eq. 31)}$$

There are two terms, then, that must be defined in order to calculate this factor, the slot opening b_0, and the stator slot pitch, τ_s. The slot opening is calculated from:

$$b_0 = \left(\frac{D}{2} - \frac{g_1}{2}\right)\operatorname{acos}\left[1 - \frac{n_{cwre}(d_w + t_{ins})}{2\left(\frac{D}{2} - \frac{g_1}{2}\right)^2}\right] + t_{ins} \quad \text{(eq. 32)}$$

where the terms are defined as:

n_{cwre} = number of conductors placed circumferentially in a slot
t_{ins} = insulation thickness

And where the stator slot pitch is calculated from:

$$\tau_s = \frac{\pi(D + g_1)}{N_{slots}} \quad \text{(eq. 33)}$$

The equivalent series turns is a much more involved computation and is computed by the following:

$$N_{se} = \frac{4}{\pi} K_s N_s \quad \text{(eq. 34)}$$

Where the term K_s is a factor defined as:

$$K_s = k_p k_d k_\chi k_s \quad \text{(eq. 35)}$$

This term now must be broken up into its consecutive terms. The term k_p refers to the pitch factor and is defined as the factor introduced by short pitching the winding. This factor is given as:

$$k_p = \sin\left(\frac{p\pi}{2}\right) \quad \text{(eq. 36)}$$

The term k_d refers to the harmonic distribution factor of the winding as presented in reference [1]. This factor is sometimes referred to by different names depending on the source. The harmonic distribution factor is given by:

$$k_d = \frac{\sin\left(\frac{\pi}{2q}\right)}{n_s \sin\left(\frac{\pi}{2n_s q}\right)} \quad \text{(eq. 37)}$$

The factor k_χ is called the slot opening factor and is common to all coils. It is defined as:

$$k_\chi = \text{sinc}\left(\frac{\chi}{2}\right) \quad \text{(eq. 38)}$$

where χ is the slot opening and is defined as:

$$\chi = \frac{b_0}{\left(\frac{D}{2} - \frac{g_1}{2}\right)} PP \quad \text{(eq. 39)}$$

The final term in the equation for K_s is k_s which refers to the skew factor. This factor is only accounted for if there is skew in the slots. Skew is done in order to avoid harmonics due to the alignment of teeth on the rotor and stator. As the rotor is smooth, skew in this machine is unnecessary and thus k_s will be 1 in this case.

3.3 Leakage Inductance

For desirable behavior in a machine, it is necessary that the leakage terms are as small as possible while the magnetizing term is large. These leakages can be divided into the following:

a. Primary slot
b. secondary slot
c. zigzag
d. belt
e. skew
f. coil end
g. incremental
h. peripheral

The total end winding leakage is made up of the coil end, incremental and peripheral leakages. The primary slot leakage is the leakage due to the slots and is given by:

$$L_{ls1} = \boldsymbol{\mu}_{effsl} \frac{4qwP_{s1}N_{se}{}^2}{N_{slots}} \quad \text{(eq. 40)}$$

Where:

μ_{effsl} = constant term as defined by Alger [2] ($12.57 \cdot 10^{-9} \frac{H}{cm}$)

And where the term P_{s1} is the total slot permeance ratio determined from the geometry of the slot as shown in Figure 3-2:

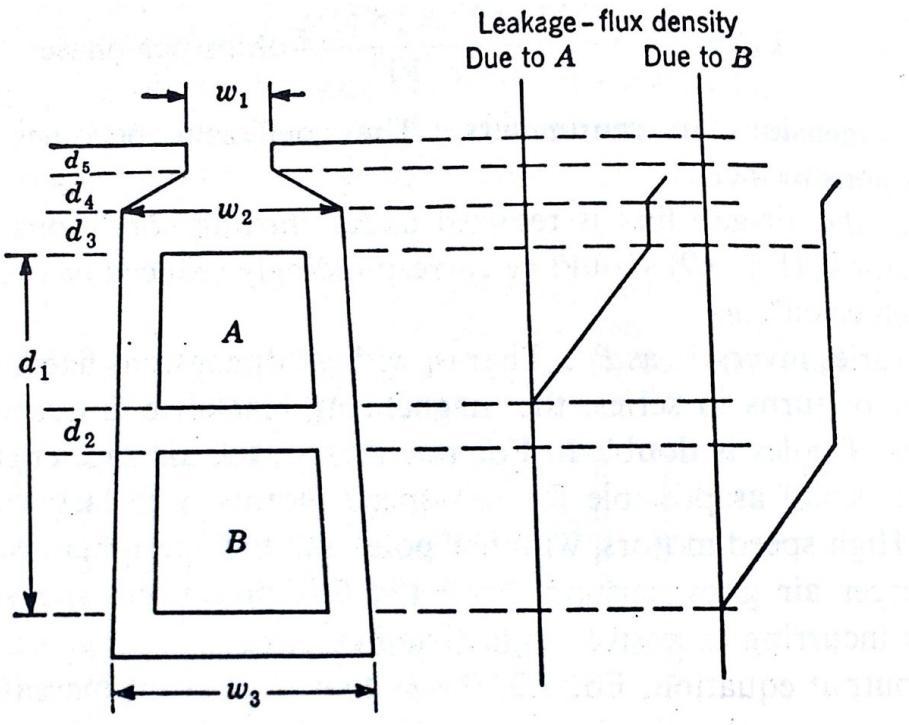

Figure 3-2: Figure 7.2 in Reference [2] for slot leakage

The slot permeance ratio is given as:

$$P_{s1} = \left(\frac{d_5}{w_1} + \frac{2d_4}{w_1+w_2} + \frac{d_3}{w_2}\right) + \frac{d_1}{3w_2} \quad \text{(eq. 41)}$$

The secondary slot leakage is the same as the primary for this application. The zigzag and belt leakages comprise what is known as the differential reactance which is caused by harmonics revolving at submultiples of synchronous speed and providing no useful result. The zigzag leakage is due to the air-gap harmonics produced if the winding had one slot per pole per phase, and the belt leakage is the additional leakage from phase belts. The zigzag leakage is calculated by:

$$L_z = \frac{\pi^2 M}{12} \frac{4PP^2}{{N_{slots}}^2} \quad \text{(eq. 42)}$$

Due to the flat-plate nature of the Image motor and the lack of coils, the belt leakage can be neglected as there are no opposing windings in which to induce circulating currents. As well, due to the lack of skew in the stator, as it is unnecessary, the skew leakage is also nonexistent. The coil end, incremental, and peripheral leakages comprise the air gap leakage. The usual pattern of the end windings and the behavior of the rotor will lead to a complicated pattern of end-leakage flux that is difficult to determine, however the total end leakage reactance formula as given by Alger in [2] is:

$$L_e = G_{alger} \frac{qD{N_{se}}^2}{(2PP)^2} (p - 0.3) \quad \text{(eq. 43)}$$

Where

G_{alger} = Constant introduced by Alger [2] ($\frac{7}{2\pi} 10^{-6} \frac{H}{m}$)

This leakage comprises all of the air gap leakages including the incremental and peripheral leakages. The total leakage will be the sum of all of these leakages and that the rotor leakage will be exactly equal to the stator leakage. From this point the lumped parameter model is fully defined.

3.4 Melcher Comparison

An analysis of Melcher's lumped parameter model for the machine discussed in Chapter 4, shows that the values of the inductance and resistance are as follows:

$R_2 = 0.556\ \Omega$

M = 25.007 mH

The values of the inductance and resistance as calculated using lumped parameters for the same machine are:

$R_2 = 0.569\ \Omega$

M = 25.309 mH

It is fairly evident that these numbers are reasonably close, and these numbers should match between the two models. The assumptions that Melcher makes in his derivation result in no stator resistance and a small leakage on the order of 0.01 mH. This small leakage is expected due to the ideal nature of Melcher's model. The mutual inductance and the resistance match, showing that the lumped parameter model is valid. Calculations of these lumped parameters are given in Appendix A, and a comparison of Melcher and the lumped parameter methods is shown in Appendix B where torque curves are given for both models.

3.5 Summary

An accurate lumped parameter model is necessary in order to do design as well as to do simulation of a machine for analysis purposes. The lumped parameter model requires a calculation of the overall resistance, magnetizing inductance and leakage inductance present in the machine. After an analysis on resistance, inductance calculations from both Lipo and Alger are presented. These calculations are used in subsequent chapters for the induction machine design.

3.6 References

[1] T.A. Lipo,*Introduction to AC Machine Design,* 3rd ed. Madison, WI: Wisconsin Power Electronics Research Center: University of Wisconsin, 2011.

[2] P.L. Alger,*Induction Machines*, 2nd ed. New York, NY: Gordon and Breach Science Publishers, 1970.

[3] J. Law, "Multiple Circuit Winding Example Solution (xmcd)," class notes for ECE 520, Department of Electrical and Computer Engineering, University of Idaho, 2013. [Online]. Available:http://www.ee.uidaho.edu/ee/power/jlaw/COURSES/ECE520 /F13/Midterm/P1Solution.xmcd. [Accessed: June 24, 2014].

4 Motor Design, Parameters, Testing and Application

The Image Motor has the potential to meet or exceed the requirements for weight and torque for a machine. In fact, at roughly 35 lbs without the tire, the hub motor will be lighter weight than any hub motor on the market today. This motor will easily provide 18 kW at 35 mph, and can be controlled with Volts per Hertz to increase speed while maintaining torque. In the following sections the Motor Design, Torque-Speed characteristics, Simulation Model, Testing and Application will be reviewed.

4.1 Motor Design

The final design of the motor involves a wound stator and a flat plate rotor. This flat plate rotor will consist of a thin wall of steel laminations which will be held together by either bolts or pressure plates. On the inside of the rotor will be a thin aluminum sheeting. This sheeting will either be adhered or powder coated onto the interior of the silicon steel tube. The aluminum sheeting will act to reflect the fields created by the stator while the magnetically permeable material will act as a return path for the magnetic fields. The stator was designed using the equations presented in Chapter 3, and is similar to that used with a squirrel cage although it is inside-out. It consists of straight teeth, wound by multiple turns of copper wire. An exploded view of the motor (stator unwound) is shown in Figure 4-1.

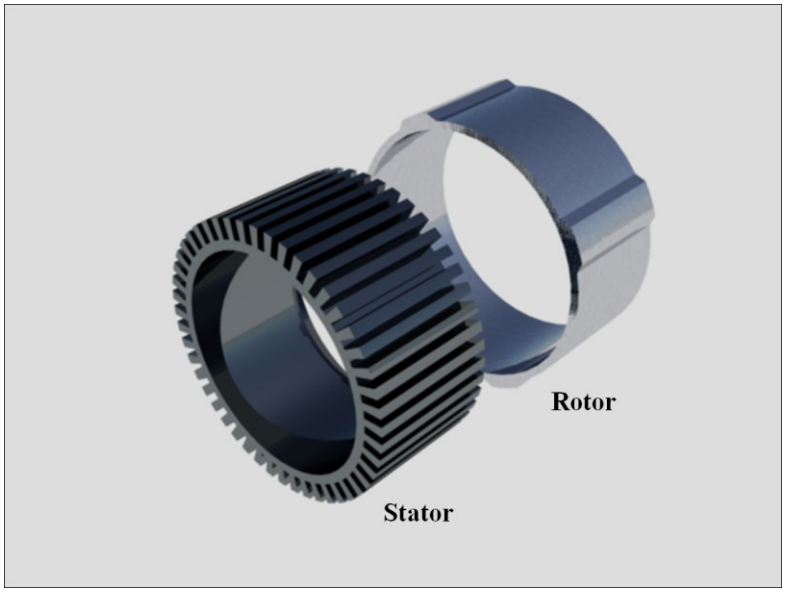

Figure 4-1: Exploded view of the IIM with unwound stator

The rotor will have a 9 inch outer diameter, with a back-iron thickness of 0.23 inches, and a conductor thickness of 0.02 inches. The rotor itself will have a length, w, of 4 inches and will be built such that it is keyed outwards at points as shown in Figure 4-2. The conducting sheet on the rotor will be aluminum, and will be either powder coated or adhered to the rotor laminations.

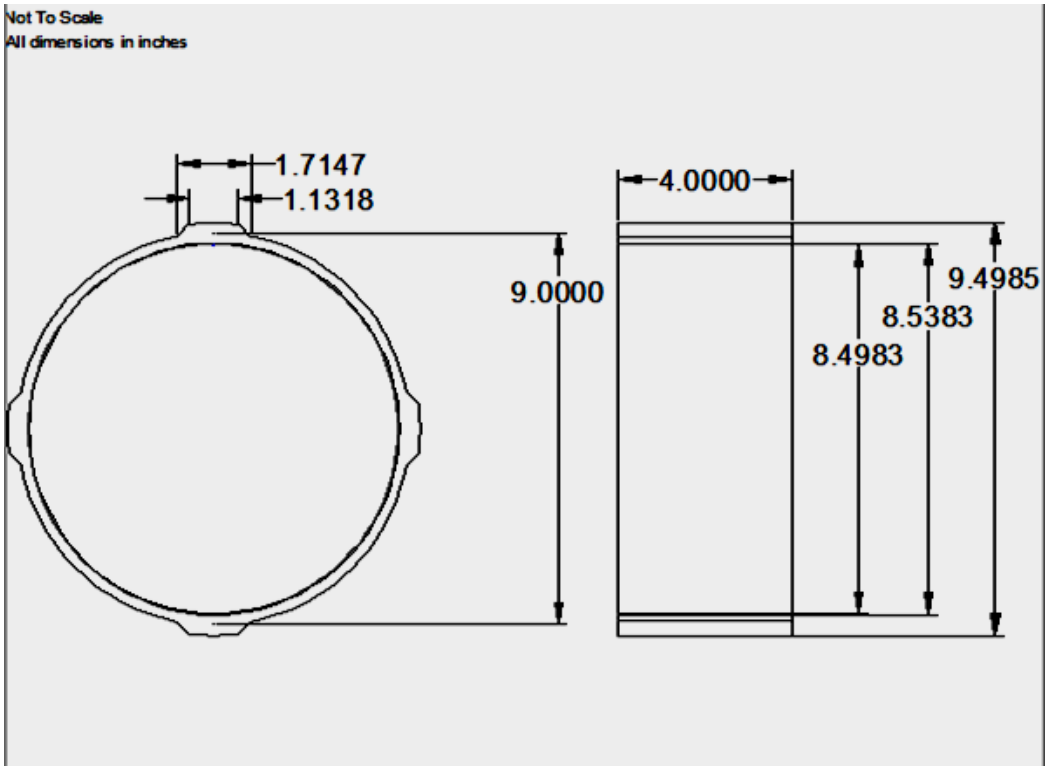

Figure 4-2: Rotor Sketch

The stator, shown in 3D exploded view in Figure 4-1, shown by itself in Figure 4-3, and shown in its full assembly in Figure 4-4 (windings not shown), has 48 slots, 4 pole pairs, and 168 series turns per phase. The dimensions for the stator and the slots, given in Figure 4-3 and Figure 4-4, are in inches.

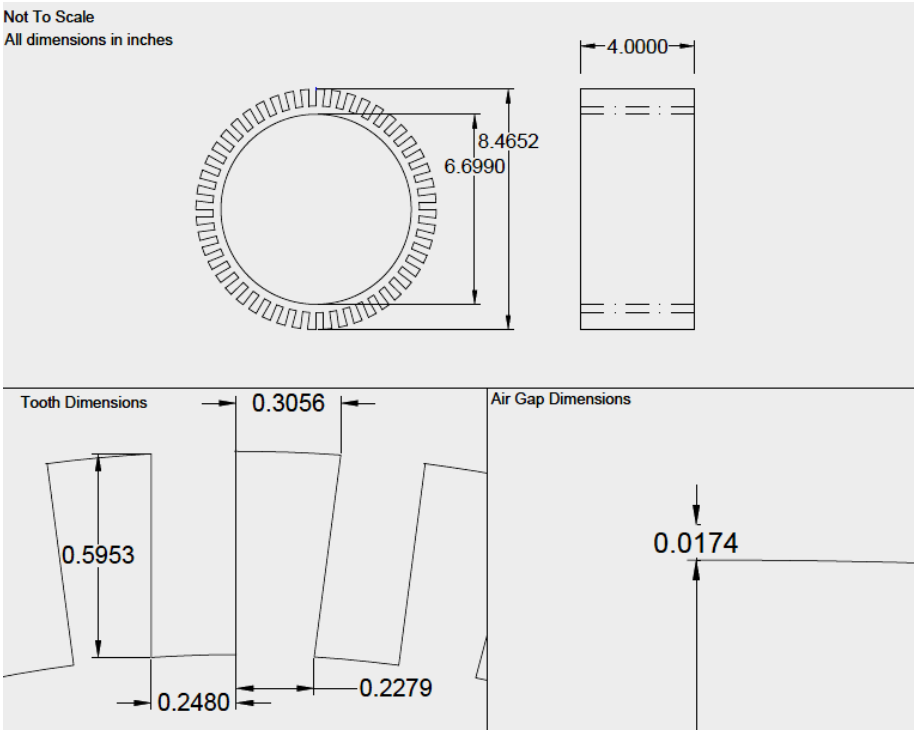

Figure 4-3: AutoCAD sketch of Stator

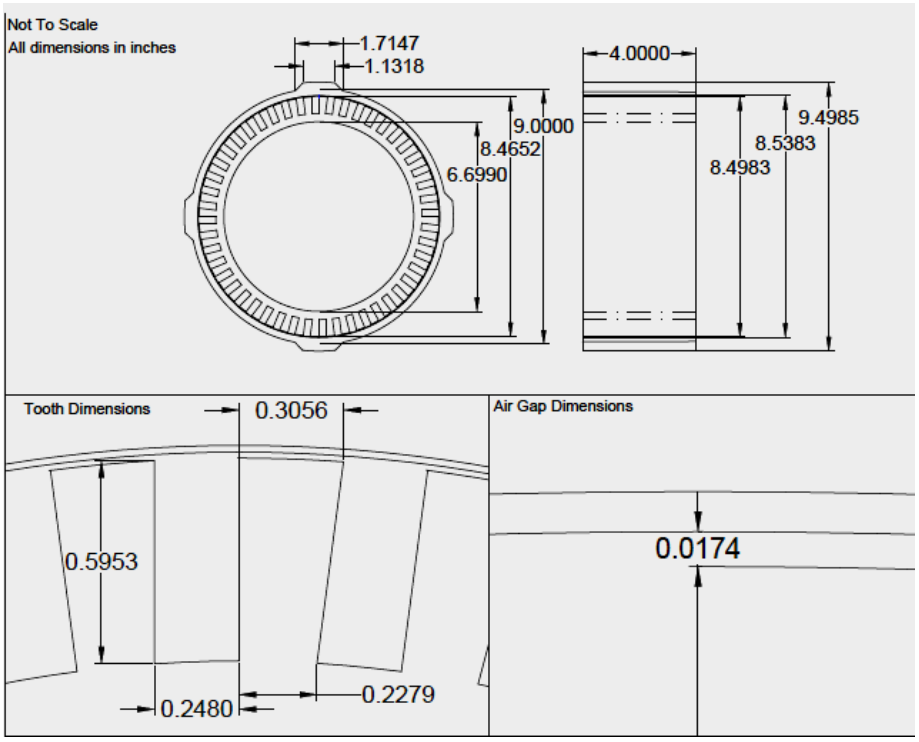

Figure 4-4: Image Motor Full Assembly

The stator will be modified slightly to account for bolts which will be installed so as to affix a stator bracket to the machine, this bracket will allow for installation onto either a test stand or car. The rotor has keys which will fit into corresponding slots within the wheel hub. This is done so that forces on the rotor do not cause the rotor to twist free of its housing during normal operation.

The advantage of this design is that there is no need for a heavy transmission or shaft which will introduce innate losses, the 200 Nm of torque appear directly on the road as the machine acts as the vehicle's wheel. Without the loss mechanisms present in the transmission or the shaft, all energy supplied to the motors minus the losses will reach the ground. As well, this particular machine only weighs 25 lbs, estimating that the entire volume of the machine is solid cast iron. When the wheel and brakes are attached, this machine will only weigh 35 lbs. This is 33 lbs less than just the machine developed by Protean Electric and this machine does not require a separate wheel housing. It should also be noted that this machine can be easily scaled up to any size wheel and horsepower without much difficulty. The machine, itself, was designed for an operating mechanical frequency of 15.083 Hz, which corresponds to 35 mph. The optimization software used to develop this machine is given in Appendix B.

4.2 Torque Speed Characteristics

The lumped parameter model for this particular machine, shown in Figure 3-1, and developed using the concepts presented in Chapter 3 gives the following parameters:

$R_1 = 0.569\ \Omega$
$R_2 = 0.369\ \Omega$
$L_1 = L_2 = 1.608$ mH
$M = 25.307$ mH

The operating voltage of the machine is 500V, the operating electrical frequency is 60.233 Hz, and the power output is roughly 18 kW at a slip of roughly 5.3%.

Using the lumped parameter model above, it is possible to calculate torque curves for the machine. Figure 4-5 shows the torque behavior of the machine during normal operation:

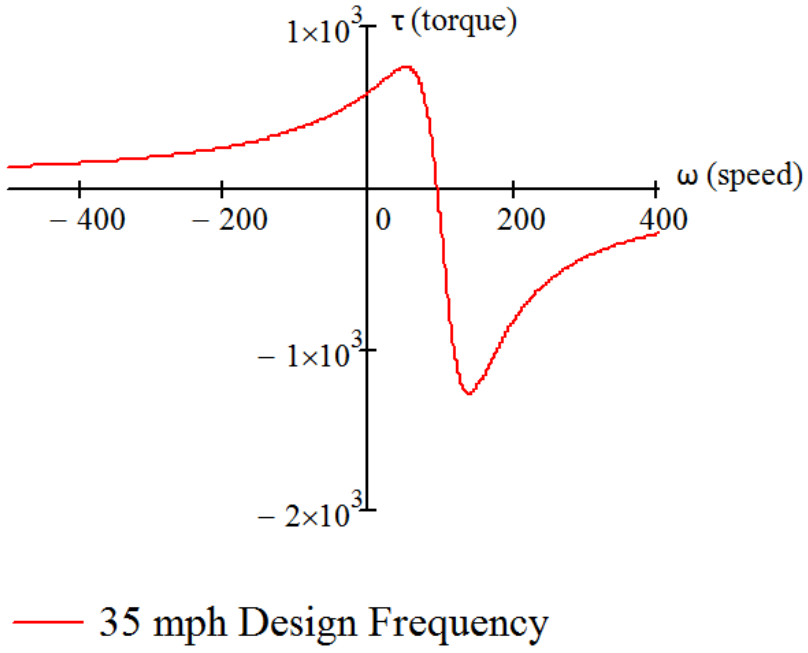

Figure 4-5: Torque Versus Speed For 35 mph Design Frequency

Appendix A provides a design sheet which shows the comparison of this lumped parameter model with the lumped parameter model provided by Melcher. When leakages for an ideal stator are accounted for the torque curves are identical, this shows the validity of the models.

The torque curve shows that this machine can easily provide the 200 Nm of torque necessary for motoring. As well, the graph shows that the machine can easily provide up to 500 Nm of torque during motoring,, and beyond 1000 Nm of torque during regeneration. It should also be noted that as frequency decreases in this machine, the machine can provide more generating torque, in essence slip will become less and less energy will be lost, meaning that efficiency will increase. This is seen in the Volts per Hertz graph in Figure 4-6. For the short time that the machine will be handling a higher current the machine should be able to handle it. This is due to the fact that it will need to decrease from 35 mph to standstill in roughly 2 seconds.

As well as having a fairly good behavior for regeneration, the machine also provides a decent behavior when increasing speed as is also shown in Figure 4-6.

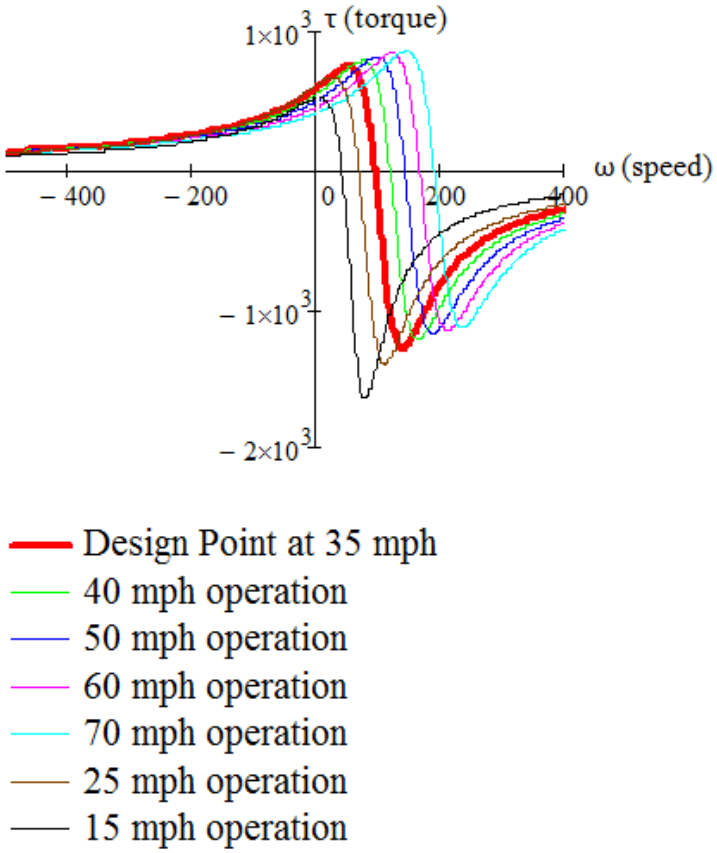

Figure 4-6: Torque Curves for different operating frequencies

The relatively flat nature of the curves shows that for increased speed, torque and power can be kept relatively constant. This also means that the machine can be easily scaled up to higher speed given the correct control while keeping a constant torque. The machine also provides a peak efficiency of roughly 88 % while providing 200 Nm of torque at 35 miles per hour, and will provide similar efficiency as torque and speed is varied

4.3 Simulation Model

The model used to simulate this machine is found in Lipo and Novotny's book, Vector Dynamics and Control of AC Drives [1], on page 60. Analysis was done in the dq reference frame, and torque, speed, and stator currents were displayed. Simulation was done using Simulink® and the model was set up so that blocks for a controller and a mechanical model. Figure 4-9 through Figure 4-17 show the different steps of the model.

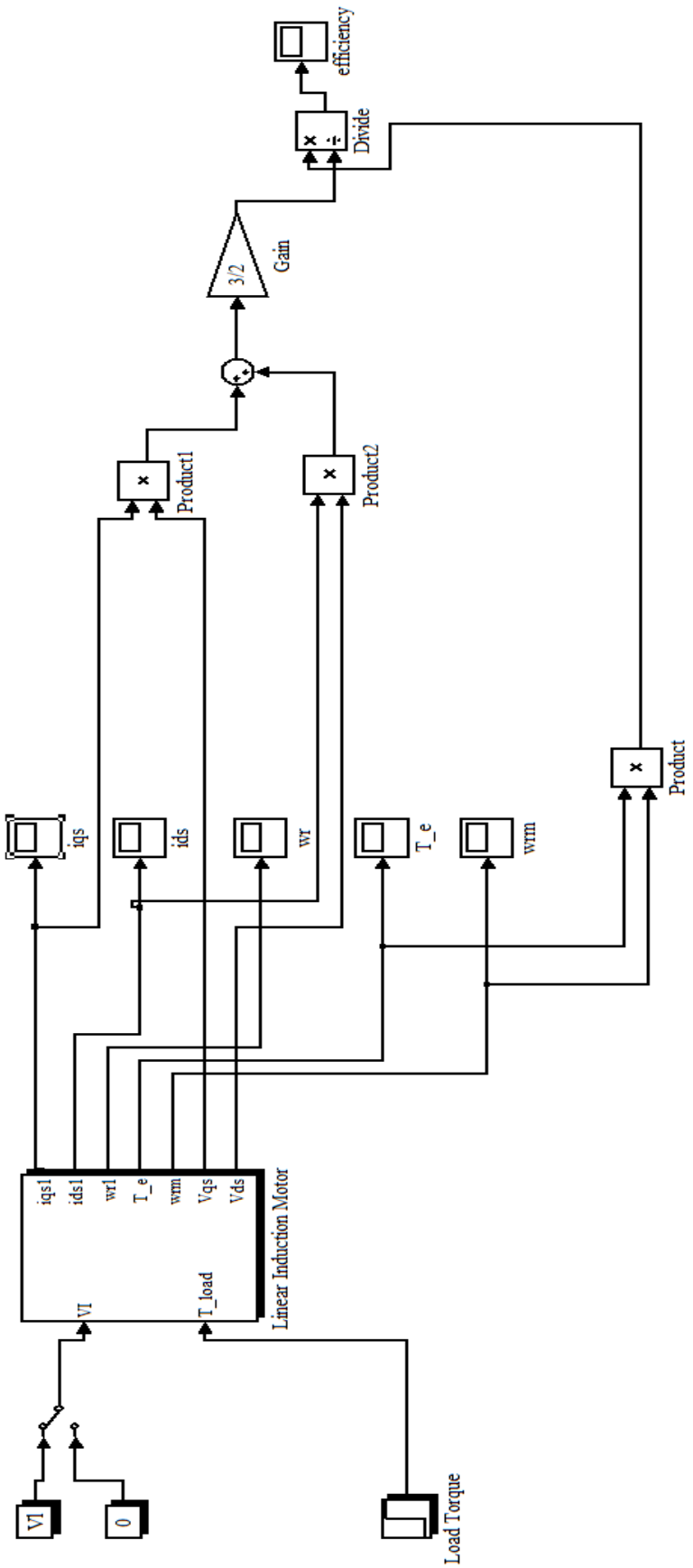

Figure 4-7: Top level of Simulink

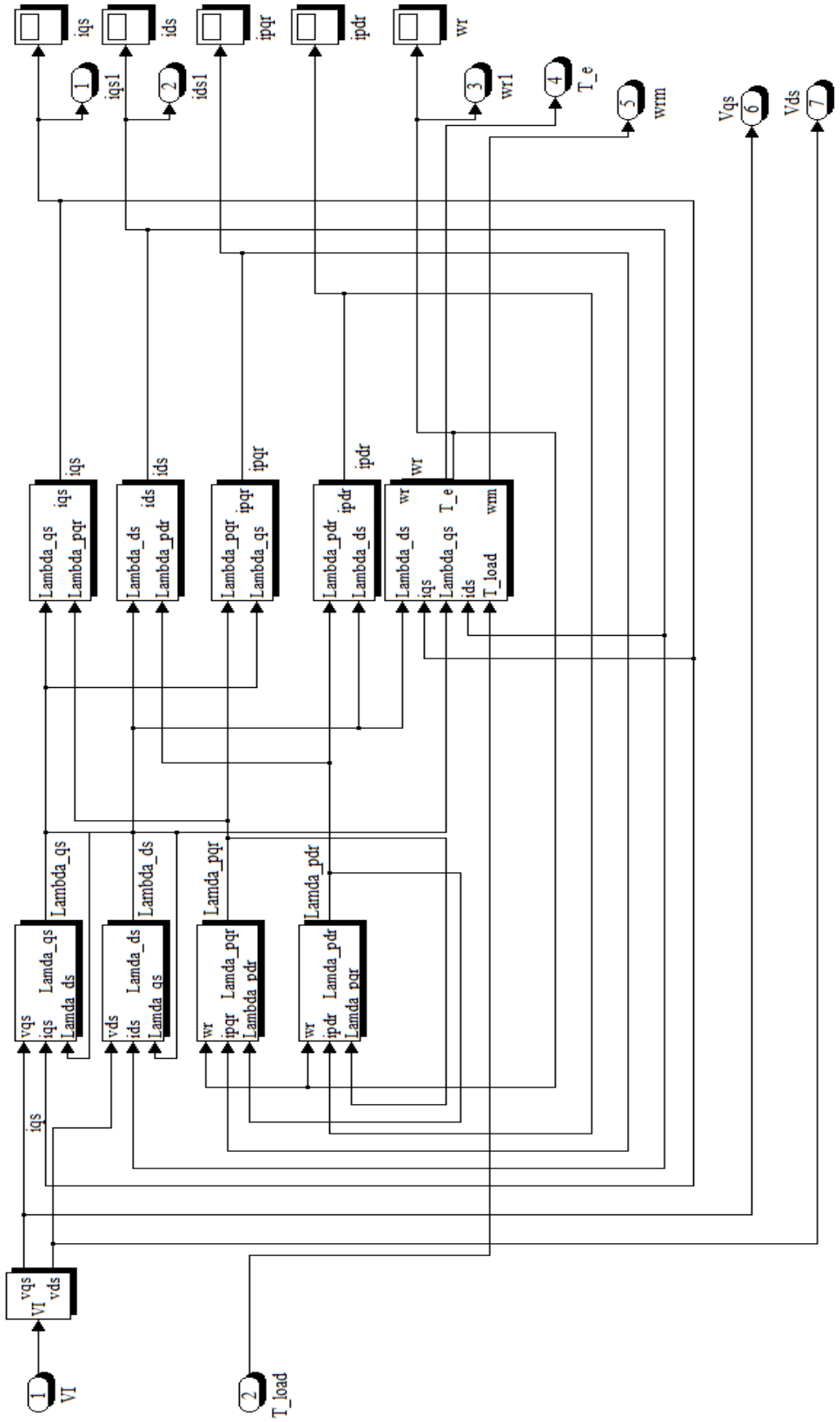

Figure 4-8: Linear Induction Motor Block

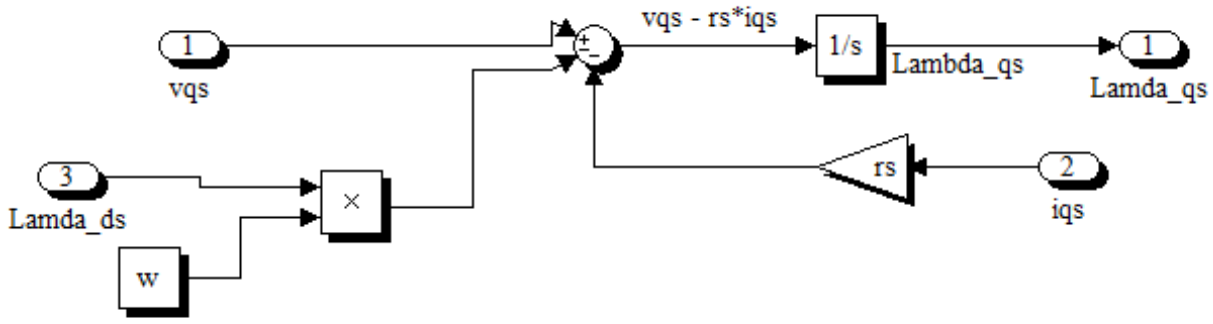

Figure 4-9: Lambda_qs block

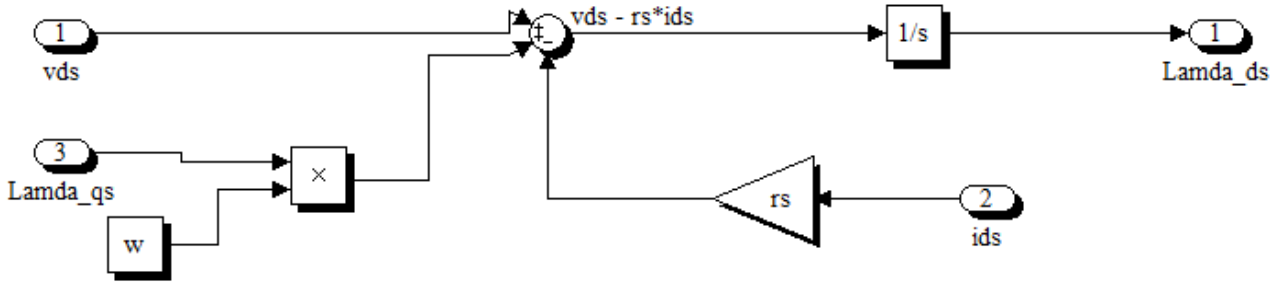

Figure 4-10: Lambda_ds block

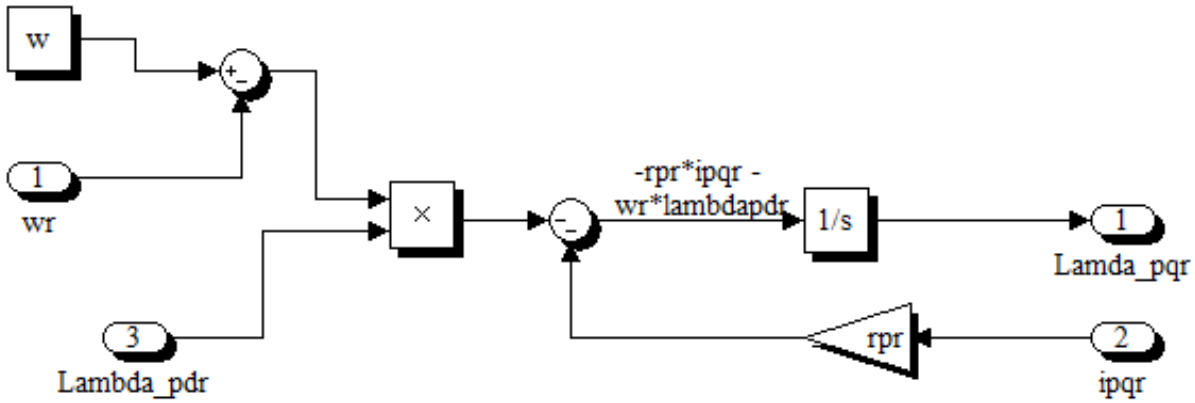

Figure 4-11: Lambda_pqr block

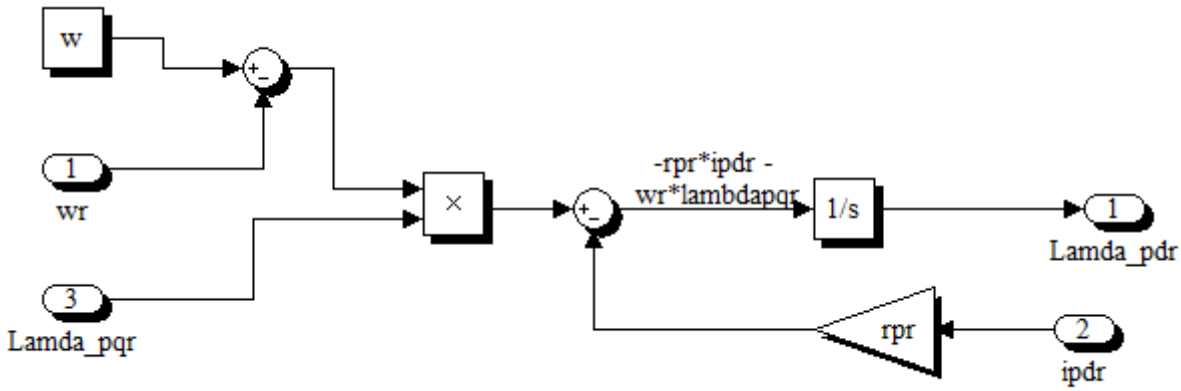

Figure 4-12: Lambda_pdr block

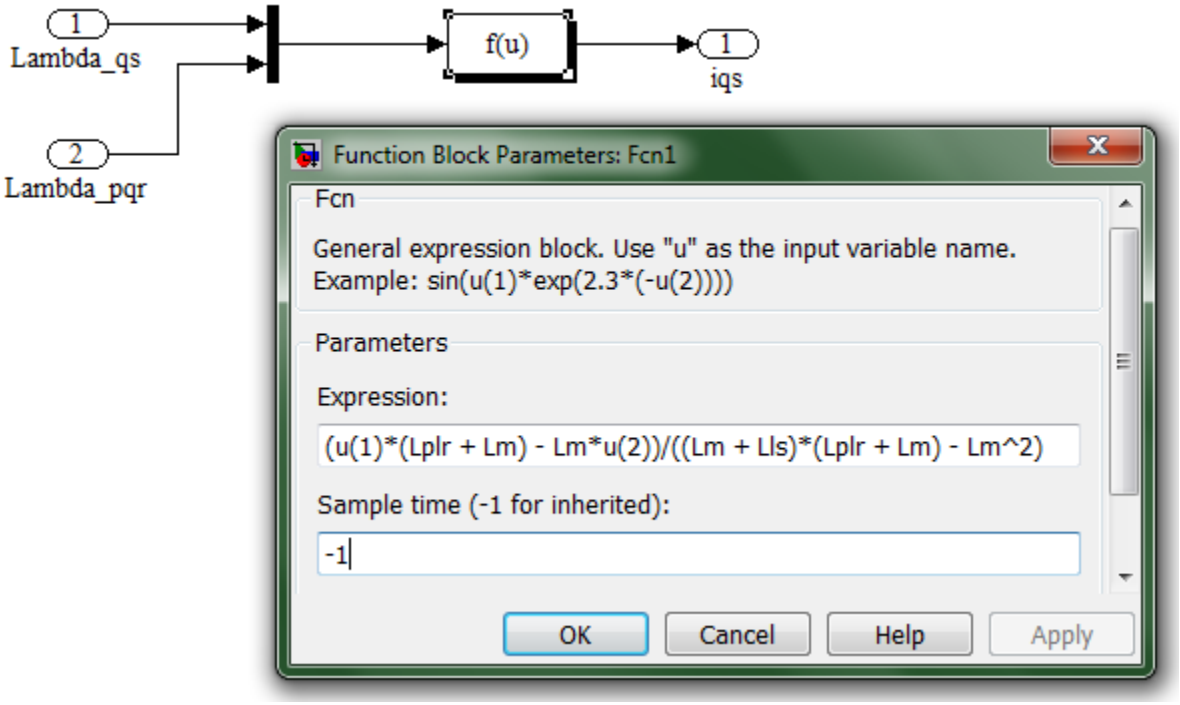

Figure 4-13: iqs block

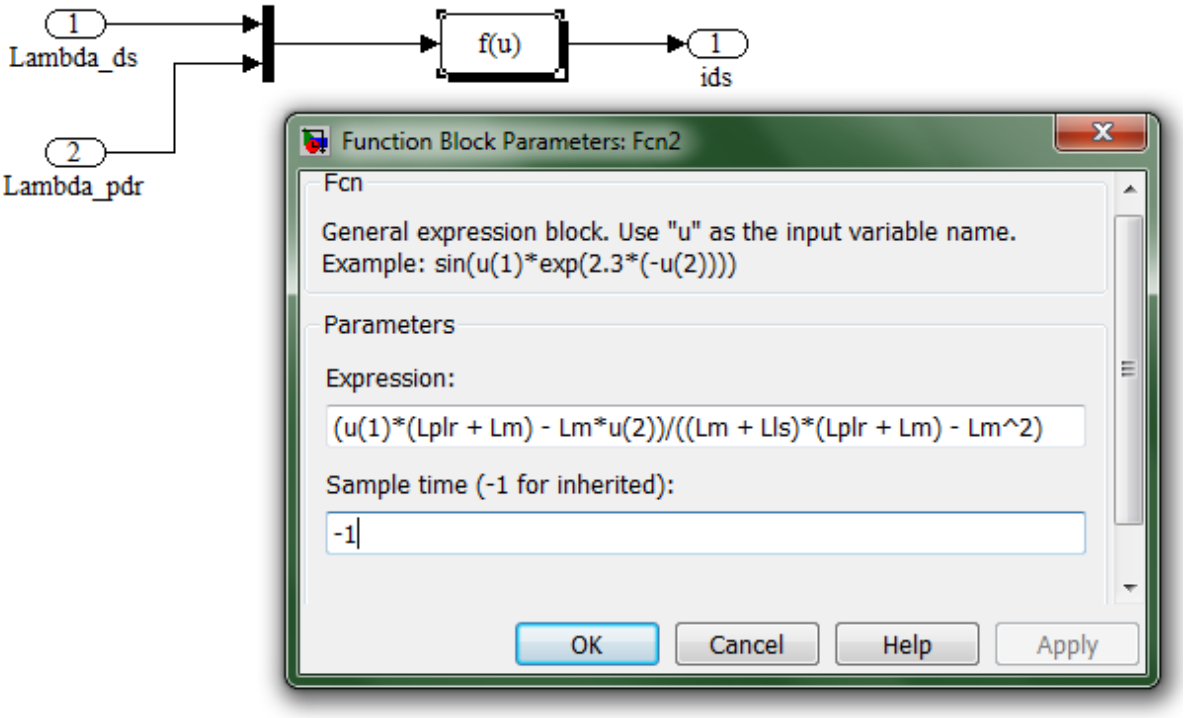

Figure 4-14: ids block

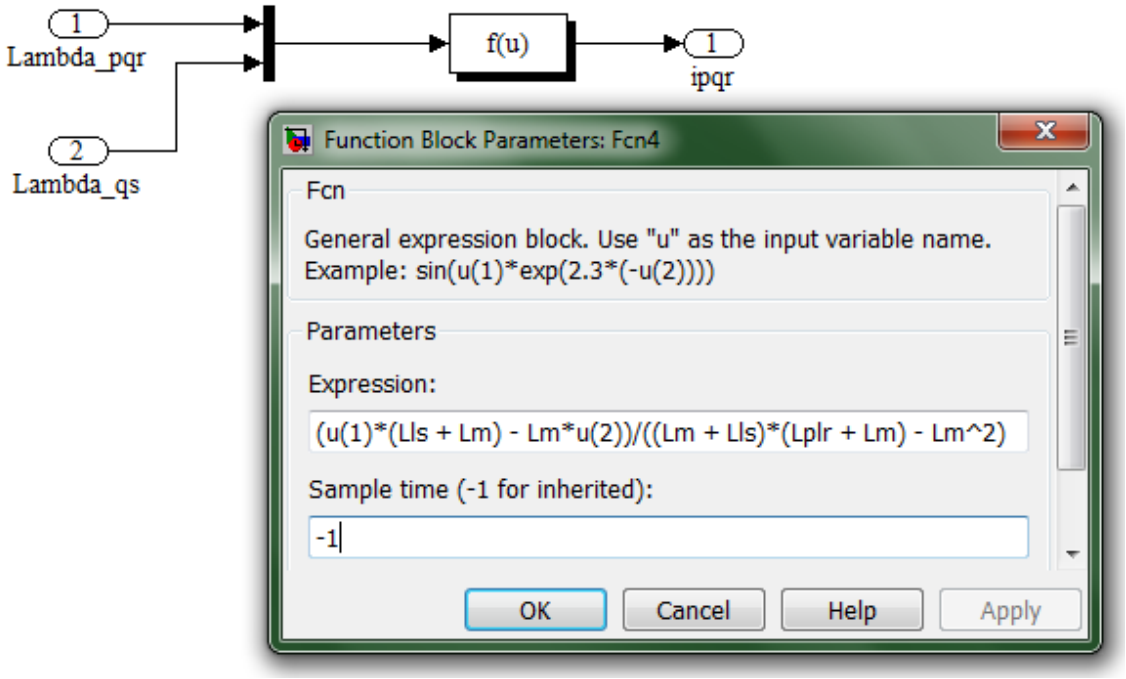

Figure 4-15: ipqr block

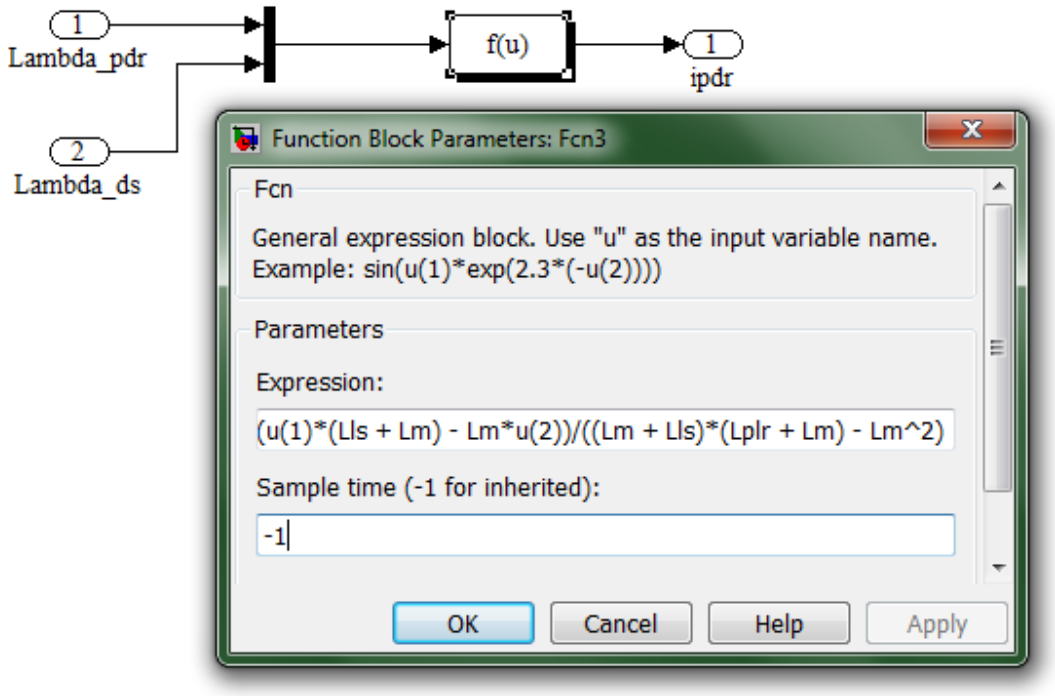

Figure 4-16: ipdr block

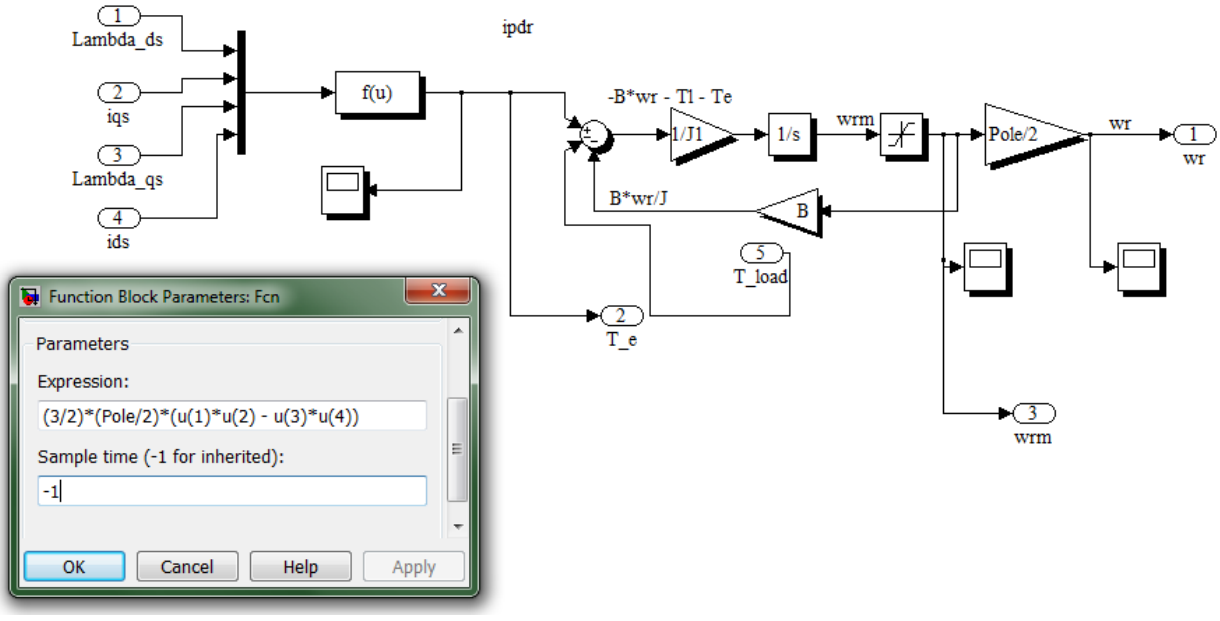

Figure 4-17: Torque and Speed Block

The MATLAB code used to generate the parameters used is given in Appendix C. The motor was provided with a 500V input, and a 200 Nm load torque was applied at 1.1 seconds after having been line started. The following plots show the motor's behavior when placed under these conditions.

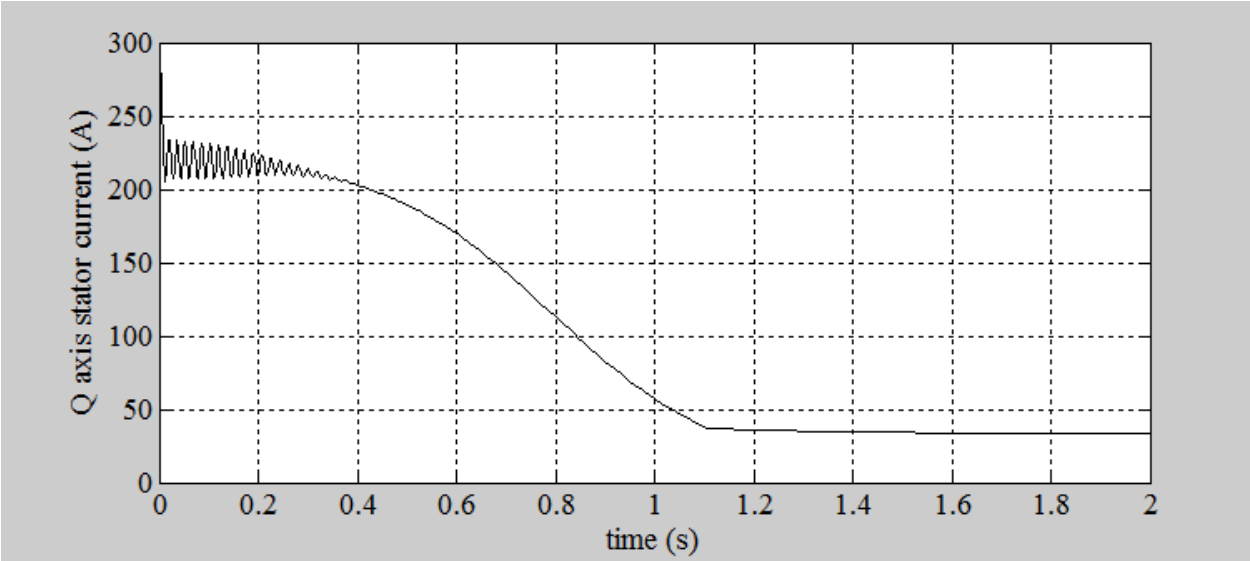

Figure 4-18: Q-axis stator current after startup

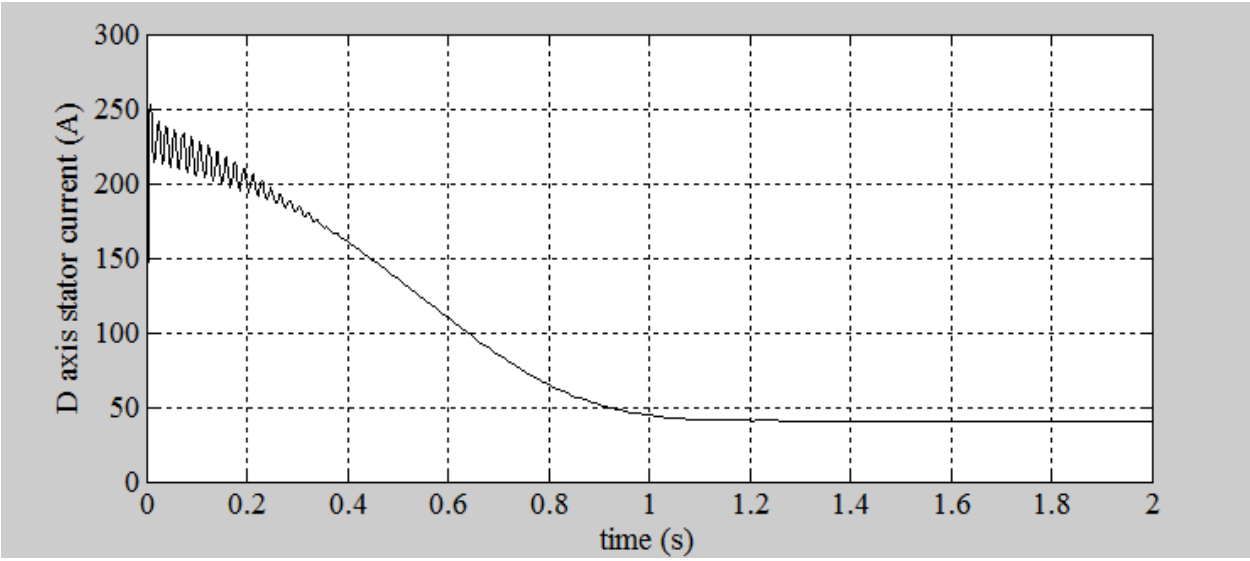

Figure 4-19: D-axis stator current after startup

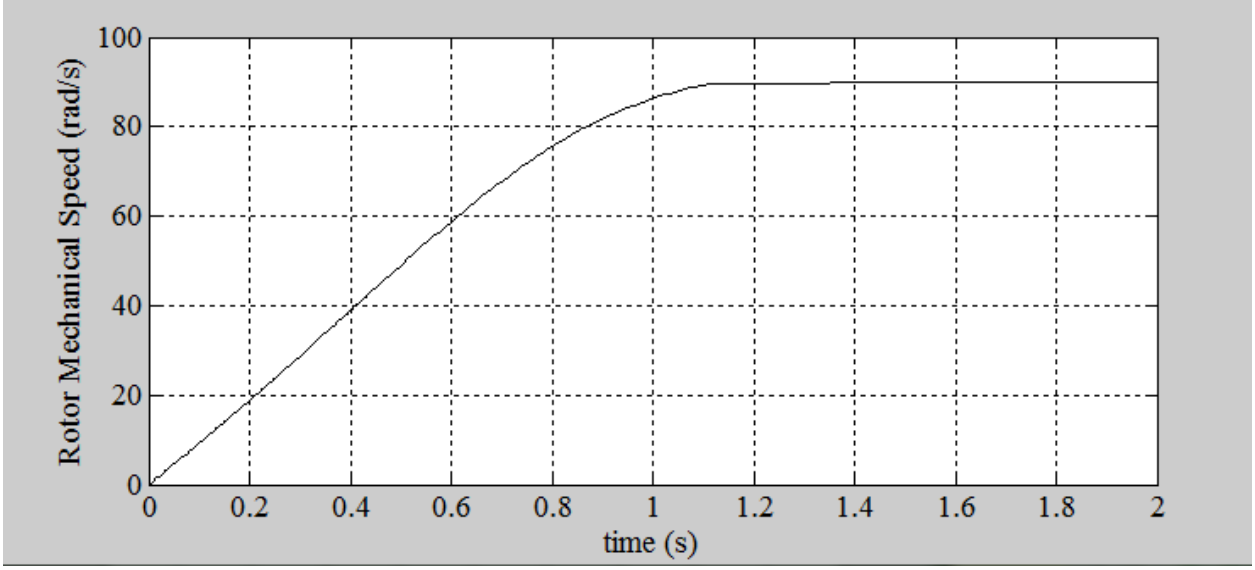

Figure 4-20: Mechanical rotor speed after startup

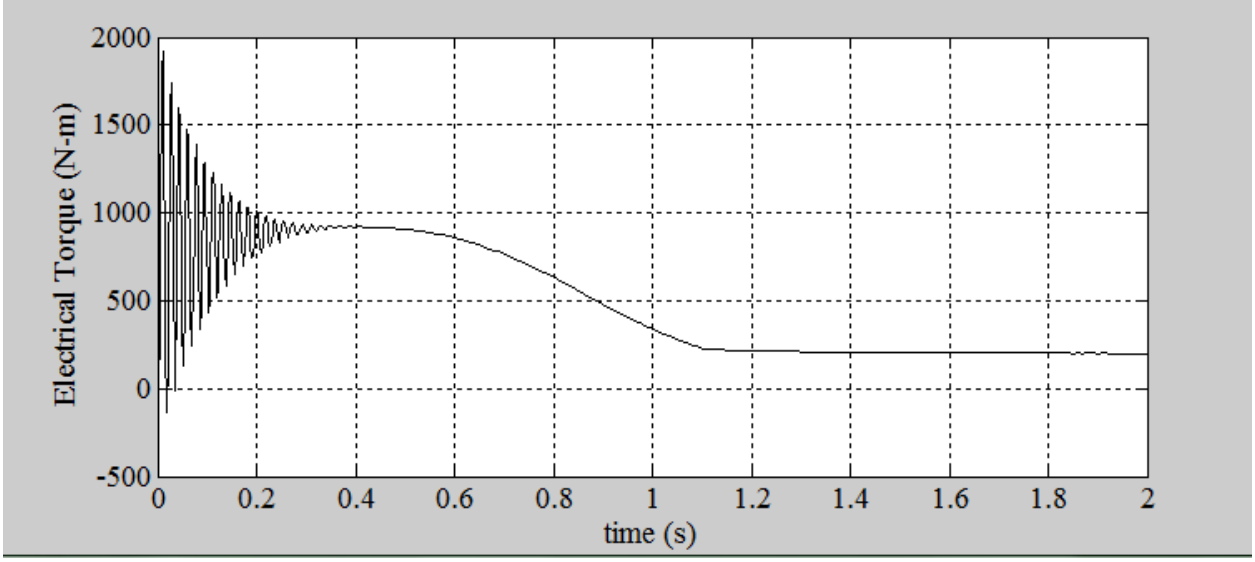

Figure 4-21: Torque response after startup

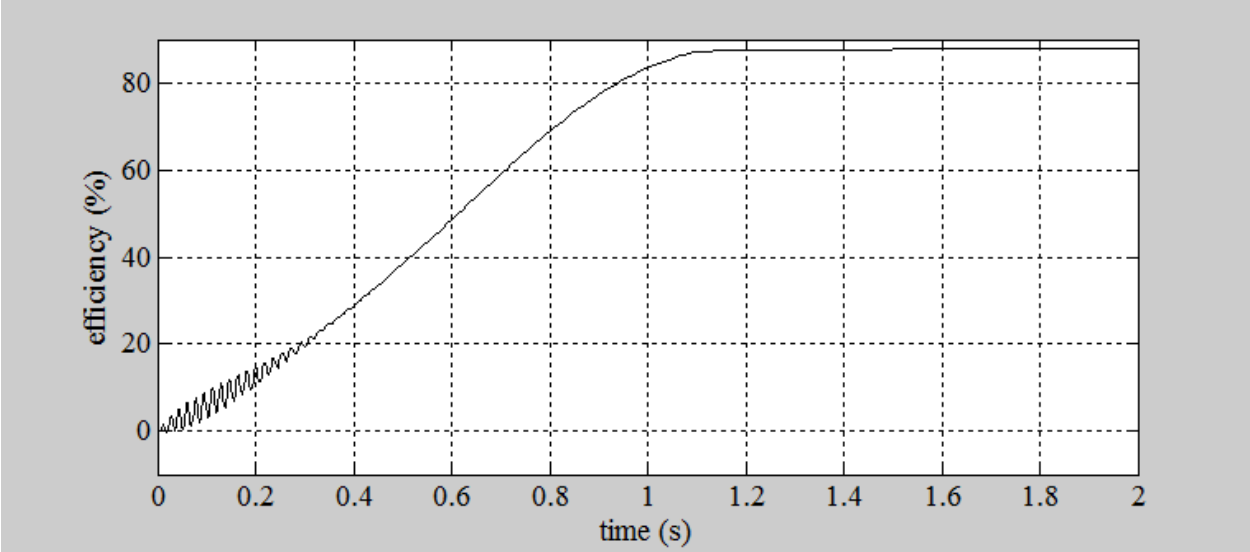

Figure 4-22: Machine Efficiency

As can be seen from the figures, when line started, the machine has a fairly fast, fairly transient response. This transient behavior is undesirable, however this can be managed through the control system and must be accounted for there. As well, the graphs show that the machine provides the desired efficiency, the desired mechanical speed, and the required torque. Further modeling will include an in-depth controller and mechanical model which can simply be built and dropped into the existing motor model.

4.4 Testing

Only so much can be determined from simulation and modeling. The existing computer models, while beneficial, cannot provide an accurate representation of how the machine will behave once built. In order to better understand the machine and its characteristics, testing is required. This testing is usually done for two main cases, the unloaded and loaded case. The following paragraphs will discuss standard testing and its incompatibility with this motor, and how this motor will actually be tested.

During standard machine testing a motor is directly coupled to another motor. This is shown in Figure 4-23:

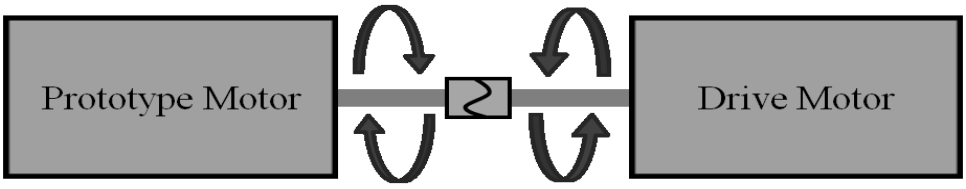

Figure 4-23: Standard machine test setup

In such a test setup, the prototype motor is driven in one direction while the drive motor is driven in the other. This applies a load torque to the prototype motor and simulates normal operation in the lab.

Due to the inside-out nature of the Image Motor and its direct-to-ground characteristics, there is no shaft to couple to a drive motor or dynamometer in order to simulate loaded operation. Thus in order to test the motor, a testing apparatus must be set up so that the motor can be loaded. To this end, a senior design team was created to design a test set up for the Image Motor.

There were several problems that the team faced when creating their stand. The unusual design of the machine did not easily lend itself to standard bearings, yet the machine needed bearings in order to maintain the air gap and keep the rotor and stator centered. The machine also needed a means by which it could be attached to a test stand or a car. In a standard machine, bolts would be placed on the outer housing in order to hold the motor to a stand. However in this machine there was no outer housing, so the team had to devise one.

The optimal solution would have involved creating a new type of inside-out wide bearing that could be either bolted to or built around the motor. Unfortunately such a solution is costly and requires increased time for design. In order to avoid the extra cost and design time, the team chose to use standard design techniques so as to keep costs down and keep as much machining in house as possible. Their solution involved installing the machine on a shaft. This allowed them to use standard bearings and to design the housing in the time allotted. In order to use a shaft two separate wheel centers had to be created, a static and a dynamic wheel center. The static wheel center would be fixed to the shaft and bolted through the stator, while the dynamic wheel center would connect directly to the wheel housing and would be press-fit

with bearings which would be pressed onto the shaft. This would allow the rotor to freely rotate while the stator remained stationary.

In order to test the motor, a belt-drive solution was devised. This solution involved fixing a gear to the outside of the rotor which would then be connected via a chain drive to a smaller shaft with a gear which would be rotated by either another motor or a dynamometer. This allows the motor to be loaded for load testing. For a no load test, the chain can be removed and the motor can be allowed to freely rotate on the shaft. The test stand setup is shown in Figure 4-24.

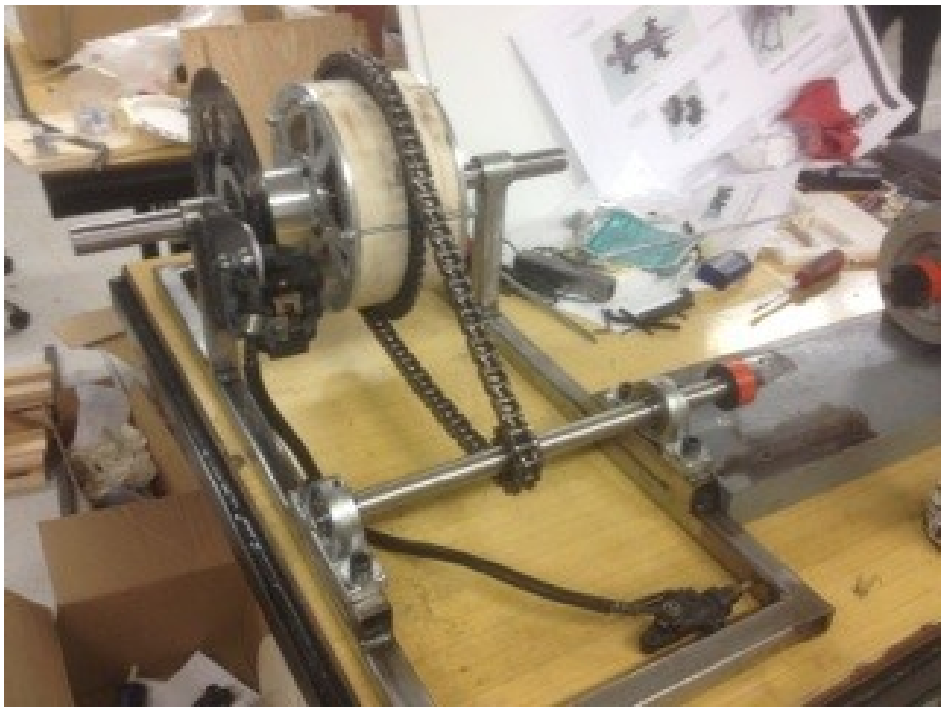

Figure 4-24: Final Assembly with wood mock up of the motor

The test stand was set up with a wooden mock up of the motor and a small motor in order to show operation and to test the brakes which will be discussed in the next section. For actual testing a different bracket will need to be built which will couple the test stand to a dynamometer which can be set to load the machine. The design of this setup can be found in the senior design team's final report which is listed as reference [2].

4.5 Practical Application

In addition to development of the test stand, the senior design students were tasked with developing a wheel which could directly attach to the motors. Because of the direct drive nature of the machines, the motor must be built into the wheel. As well, a backup mechanical brake had to be created so that in case of machine failure the vehicle could still be brought to a stop.

The senior design team created a wheel design that includes wheel barrels and a standard brake. This brake and wheel barrel assembly utilizes the same setup as the test stand. The wheel design is shown in Figure 4-25 and Figure 4-26.

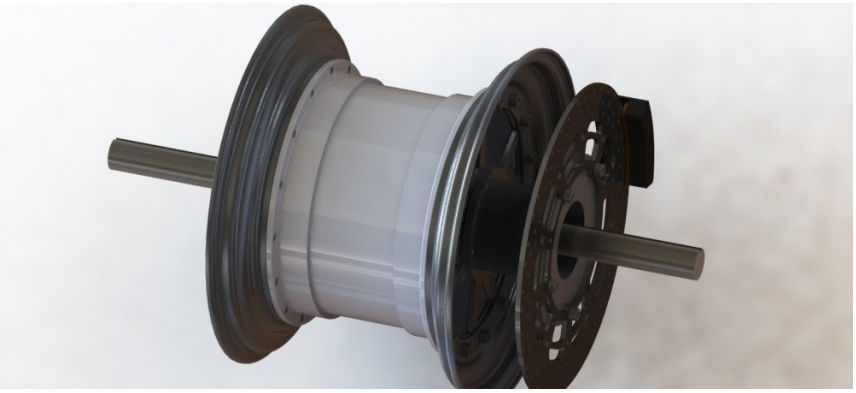

Figure 4-25: Solidworks mockup of full assembly

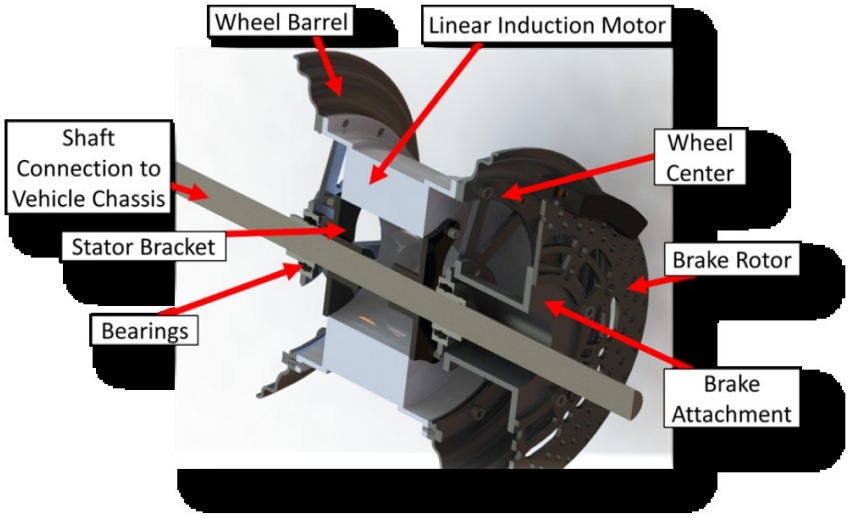

Figure 4-26: Cutaway of full assembly

In order to place this on a car, some modification will be required so that the wheels can operate independently. However, that is the topic of another thesis or senior design project.

It is important to note that the designs above were done in the short term and on a small budget, thus in order to decrease weight and increase efficiency it is necessary to re-think how these wheels are designed. The senior design team discussed building a wide bearing that would be bolted to both the stator and rotor, however the development would take time and finances they did not have [2]. Another option would be to build a bearing housing, as shown in Figure **4-27** below.

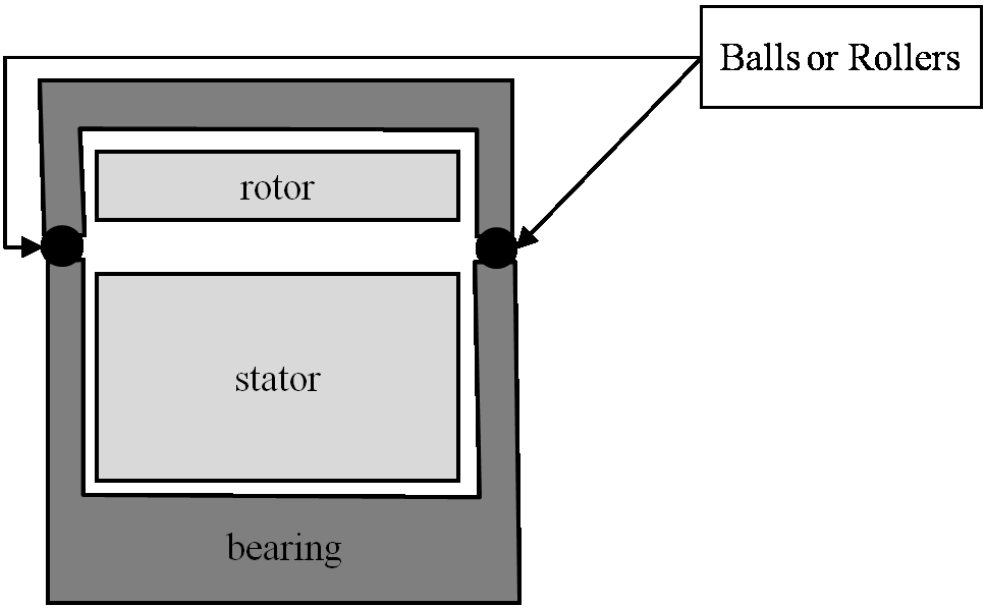

Figure 4-27: Bearing Housing Idea

This housing would act as the casing for the motor, and would also act to protect the rotor conductor and stator conductors from damage. As well, a casing of this kind would decrease the overall weight of the machine and its housing. A variation on this idea would require further research and funding, and would be the topic of another mechanical engineering project.

4.6 Summary

This chapter covered the design and layout of the rotor and stator, the torque-speed characteristics, the simulation model, testing and practical application. From a careful analysis

of the motor it is evident that this machine provides better torque characteristics than most squirrel cage induction motors and will work better for motoring and generating than the DC and synchronous machines currently being used. As well, the Image Motor provides a lower weight than any machine on the market today, bringing the total weight of the motor and wheel assembly down to 35 lbs which is on-par with the weight of a standard wheel. There is still much research to be done on this topic, and some of the topics for further research will be discussed in chapter 5.

4.7 References

[1] D.W. Novotny and T.A. Lipo, *Vector Control and Dynamics of AC Drives,* Oxford, NY : Oxford, 1996.

[2] J. Nair, T. Bischoff, M.Wilson, V. Zarate, and C. Subhedar, "All Electric Vehicle Powertrain", Senior Design Report, University of Idaho, Moscow, ID, 2014.

5 Conclusions

Standard electric vehicles do not meet consumer demand due to their relatively short range and long charging times. This range issue is caused, in part, by the choice of motor and powertrain topology. In a standard powertrain the losses and added weight of a transmission significantly decrease overall vehicle efficiency, this inefficiency has led many to consider development of a direct drive motor. There are several drawbacks to the standard direct drive motors, as electric vehicle manufacturers have constrained themselves to permanent magnet DC and synchronous machines. This has led to motors weighing between 68 and 350 lbs, which places high un-sprung mass on the wheels. As well, depending on the size of these machines, the weight can defeat the very purpose of direct drive.

The image motor solves many of the problems with direct drive motors. By using a thin aluminum plate and multiple poles on the stator, it is possible to bring down the weight of a motor to between 25 and 40 lbs. This is done by utilizing a thin plate aluminum rotor and a high frequency on the stator. A machine of this type is typically designed using finite elements, however standard design techniques can be used.

It is possible to design the image motor using standard design techniques when analyzed in the context of image conductors. This theory states that the stator winding will produce an image of itself on the rotor plate which will result in an equal inductance and proportional resistance on the stator and rotor. When continuum mechanics is used to analyze the same type of machine, results are obtained that are equivalent to those obtained through these standard design methods. This is further discussed in Chapter 2 and Chapter 3.

The machine which was designed using the standard design techniques presented in Chapter 3 provides an 88% efficiency while at the same time maintaining a total wheel assembly weight of under 40 lbs, the design and application of this machine is given in Chapter 4. It is important to note that this machine was designed for a half-scale formula car and an outer diameter of only 9 inches. A larger diameter will allow for a higher power machine of a similar weight for a full scale vehicle.

In order to apply this machine, there are several things that still need to be done. A prototype of the machine still needs to be built and tested in a lab, then tested on a car. Further research will then be required to bring down the weight of the motor, and increase the motor's overall efficiency. And finally a full statistical study needs to be done in order to determine what exactly needs to be done in order to make electric vehicles viable.

5.1 Motor Prototyping and Testing

The next step with this motor involves building and testing a prototype. This prototype will be built by one of various motor manufacturers around the area. This will then be installed in the test-stand built by the senior design students and tested using IEEE STD 112. Load testing will be done by building a bracket to connect to the dynamometer, and the dynamometer will be used for the load test.

For the next series of tests there are several mechanical designs that need to be evaluated and completed. The motor housing used for the test stand will work fine for in-lab work, but when applied in the elements they may not be up to par. In order to remedy this, a new motor housing will need to be built, either adapting the senior design team's test stand setup or building a "bearing housing" which would keep weight down. As well, there are several environmental concerns that need to be addressed before a motor is applied to a wheel.

Due to the location of the machine and its exposure to the elements, it could see uneven heating and potential damage due to thermal expansion. To check for issues that this may cause, exposure to sunlight for a prolonged period of time needs to be simulated and the machine needs to be tested under increased temperature conditions such as what may be seen on a hot summer day.

In addition to thermal concerns the machine also needs to be able to withstand stresses it may encounter during rain or snow, for that purpose both of these conditions need to be tested and functionality of the machine should be verified. As well, the machine will be subject to vibrations on the road, and for this reason it will need to be tested for any issues associated with road vibrations. These tests will need to be concluded prior to the machine's installation on a vehicle.

5.2 Future Motor Work

The current motor only has an 88% efficiency. This is partially due to the light-weight nature of the machine. A slightly heavier machine will see an increase in efficiency as a heavier machine allows for more iron and thus deeper slots. One way to increase the efficiency without increasing weight would be to use a different geometry on the slots and teeth. The teeth on the machine discussed in this thesis were designed such that the slots would be a straight rectangle. Considerable research has been done regarding the effects of various slot geometries, and the application of one of these geometries to the image motor could result in an increased efficiency. In order to simplify analysis for this machine series windings were used. The application of parallel windings could potentially decrease resistances and thus decrease resistive heating losses. This would also result in an increased efficiency.

In several papers it has been postulated that a back iron is not necessary if a thick aluminum rotor is used. A simple test of this would be to replace the rotor for the initial prototype with a solid aluminum rotor of the same shape. If this produces the same torques and a similar efficiency, this could further decrease the weight of the machine, as aluminum has a lower density than steel.

5.3 Electric Vehicle Application

The design created by the senior design team is optimum for a test stand, however further research needs to be done in applying these motors to electric vehicles. Wheels can be made lighter by creating large bearings that would encompass the motors, in other words building a sort of "bearing housing" for the motor which could then be bolted into wheels. This idea was discussed both by the senior design team, and discussed in more detail in chapter 4. Even using the senior design team's test-stand motor housing, it is necessary to design a new type of suspension. This suspension would require reinforcement to withstand the applied torque in both the body of the vehicle and the motor. This leads into the need to re-design the vehicle's undercarriage.

In addition to requiring further mechanical design for connecting these motors to a car, several controllers need to be built. The first controller would be the motor control. For a first permutation, this controller could be a modified version of a commercially available

controller. For increased efficiency and better control it is necessary to design a controller specifically for the image motor. This controller will need to be able to control both motoring and regenerating and will require further research.

An overall control scheme needs to be built that will govern the overall operation of the vehicle. Tasks for this control scheme will include coordination of the four separate motor controllers, appropriate commands based on throttle and brake inputs, and commands based on steering. The electrical design of this control system will require a computer or electrical engineering design team. In addition to the electrical design, a mechanical design team is required to define the dynamic system and determine the commands that will be issued to the motors during operation.

As well as the direct control and installation of these motors, the battery systems can now become larger as weight has been removed from the body of the vehicle. This means that more energy storage is possible as a heavier battery system can be installed. Research into these larger battery systems is required, and further research into their optimization needs to be done. In addition to battery storage, further research into developing a regenerator specifically for these motors needs to be completed.

5.4 Future Statistical Analysis

In order to truly make a better electric vehicle, a comprehensive statistical analysis must be performed in order to determine what all needs to be done to electric vehicles in order to make them viable. Such an analysis would determine exactly how far the range needs to be extended, how quickly the car should charge from a standard outlet, what kind of infrastructure would need to be installed in order to make these plausible on a large scale, what exactly needs to be done to the electronics on the inside of a vehicle to increase range, etc. The infrastructure is a large issue, because while a few electric vehicles do not present a large draw on the grid, electric vehicles purchased on the scale of the number of U.S. cars will present a large load. Such an infrastructure study would determine exactly how much of an increase in load electric vehicles will be and how much generation needs to be added in order to compensate for the increase in load. An in-depth statistical analysis would identify the problem points with electric vehicle so that electric vehicle research can be completed with

more precision, focusing on the main problems with electric vehicles. Such a study would be invaluable to research at Universities across the country and would involve the math department, as such a study is beyond the scope of engineers.

5.5 More Applications

Along with the advances that could be made in this particular machine for the automotive industry, this machine is easily adapted to other uses. For example a new application of this machine to marine devices such as boats or jet skis may be in order. As well, this machine could be used for space vehicles as its weight is low, or it could be used for flywheels as it has a high slip and decent efficiency. Other applications may involve determining whether or not one of these machines could be used to develop lift such as that in a helicopter and whether or not the decreased weight is of interest. The uses of a lightweight machine are endless and more applications exist than presented in this thesis.

5.6 Summary

More than simply building a prototype, further research needs to be done with this motor in order to increase its efficiency and decrease its weight. As well, research by both electrical and mechanical engineers needs to be done in order to better apply these motors to an electric vehicle. Besides electric vehicles, there are many applications that could use a lightweight motor, from marine to aeronautics to space. And in addition a full statistical analysis needs to be done in order to better pinpoint what research needs to be done on electric vehicles.

Appendix A

This appendix shows the calculation of Melcher's parameters and the comparison of the torque curve obtained through continuum mechanics and the torque curve obtained through Lipo and Alger's techniques.

Defining machine dimensions

$w := 4 \cdot in$

$D_2 := 9 \cdot in - 0.25 \cdot in - 0.2 \cdot mm$ $\quad l_1 := 2 \cdot 0.174 \cdot m$ $\quad j := \sqrt{-1}$

$N_{A1} := 199 \cdot \frac{2}{3}$ $\quad N_a := \frac{2N_{A1}}{l_1}$ $\quad N_a = 762.452 \frac{1}{m}$

$l_1 = 348 \cdot mm$

$d_1 := 1.584 \cdot mm$

$s_t := 0.5 \cdot mm$ $\quad k_1 := \frac{2 \cdot \pi}{l_1} = 18.055 \frac{1}{m}$ $\quad m\Omega := 10^{-3} \cdot \Omega$

$\sigma := 3.70 \cdot 10^7 \cdot \frac{1}{\Omega \cdot m}$ $\quad s_t = 0.02 \cdot in$

defining a skin depth term

$\sigma_s := s_t \cdot \sigma$

Calculating ideal leakage inductance

$k_1 \cdot s_t = 9.028 \times 10^{-3}$

$L_1 := \frac{w \cdot N_a^2 \cdot \mu_0 \cdot l_1^2}{4 \cdot \pi} \cdot \tanh\left(\frac{\pi \cdot d_1}{l_1}\right)$ $\quad L_1 = 0.01 \cdot mH$

Calculating magnetizing Inductance

$\tanh\left(\frac{\pi \cdot d_1}{l_1}\right) = 0.014$

$M := \frac{w \cdot N_a^2 \cdot l_1^2 \cdot \mu_0}{4 \cdot \pi \cdot \sinh\left(\frac{2 \cdot \pi \cdot d_1}{l_1}\right)}$ $\quad M = 25.007 \cdot mH$ $\quad \frac{L_1}{M} = 0.041 \cdot \%$

Calculating rotor resistance (note: ideal stator resistance sets stator resistance to 0)

$R_1 := \frac{l_1 \cdot w \cdot N_a^2}{2 \cdot \sigma_s}$ $\quad R_1 = 0.556 \cdot \Omega$

Setting stator resistance to 0

$R_2 := 0 \cdot \Omega$ $\quad L_{11} := L_1$ $\quad L_M := M$ $\quad PP := 4$ $\quad L_2 := L_1$

$R_{2_{actual}} := 0.389 \cdot \Omega$ adding actual resistance of the stator to melcher's ideal machine to provide a more realistic result.

3 phase to α, β transformation

$V_{LL} := \frac{500}{\sqrt{3}} \cdot V$

$$V_a := V_{LL} \cdot e^{j \cdot 0 \cdot deg}$$

$$V_b := V_{LL} \cdot e^{j \cdot -120 \cdot deg}$$

$$V_c := V_{LL} \cdot e^{j \cdot 120 \cdot deg}$$

$$a := e^{j \cdot \frac{2 \cdot \pi}{3}}$$

calculation of alpha and beta voltages

$$V_\alpha := \sqrt{\frac{2}{3}} \cdot \left(V_a \cdot \cos(0) + V_b \cdot \cos\left(\frac{2\pi}{3}\right) + V_c \cdot \cos\left(\frac{-2 \cdot \pi}{3}\right) \right)$$

$$V_\beta := \sqrt{\frac{2}{3}} \cdot \left(V_a \cdot \sin(0) + V_b \cdot \sin\left(\frac{2\pi}{3}\right) + V_c \cdot \sin\left(\frac{-2 \cdot \pi}{3}\right) \right)$$

Setting frequency and slip terms

$$f_e := 60.332 \cdot Hz \qquad f_{sys} := f_e \qquad \omega_s := f_{sys} \cdot 2 \cdot \pi \qquad \omega_{sm} := \frac{\omega_s}{PP}$$

$$\omega_s = 379.077 \frac{1}{s}$$

calculating equivalent impedances:

$$s_m(U) := \frac{\omega_{sm} - U}{\omega_{sm}}$$

$$Z_{eq}(U) := j \cdot \omega_s \cdot L_1 + R_2 + \left(\frac{1}{j \cdot \omega_s \cdot L_2 + \frac{R_1}{s_m(U)}} + \frac{1}{j \cdot \omega_s \cdot M} \right)^{-1}$$

Calculating alpha and beta currents

$$I_{\alpha s}(U) := \frac{V_\alpha}{Z_{eq}(U)}$$

$$I_{\beta s}(U) := \frac{V_\beta}{Z_{eq}(U)}$$

$$I_{\alpha r}(U) := I_{\alpha s}(U) - \frac{V_\alpha - \left(j \cdot \omega_s \cdot L_1 + R_2\right) \cdot I_{\alpha s}(U)}{j \cdot \omega_s \cdot M}$$

$$I_{\beta r}(U) := I_{\beta s}(U) - \frac{V_\beta - (j \cdot \omega_s \cdot L_1 + R_2) \cdot I_{\beta s}(U)}{j \cdot \omega_s \cdot M}$$

Calculating electrical power

$$P_e(U) := 2 \cdot R_1 \cdot \frac{(1 - s_m(U))}{s_m(U)} \cdot \left(\left| I_{\alpha r}(U) \right| \right)^2$$

determining electrical torque for Melcher's Machine:

$$T_{em}(U) := \frac{P_e(U)}{U}$$

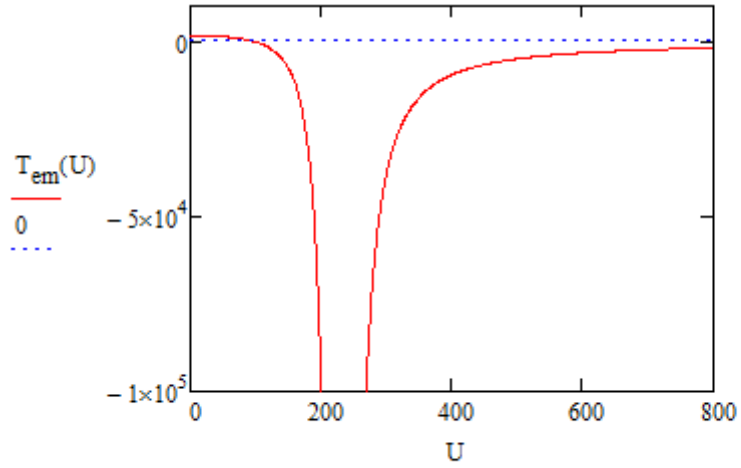

Plot of Lipo and Alger Torque for Comparison:

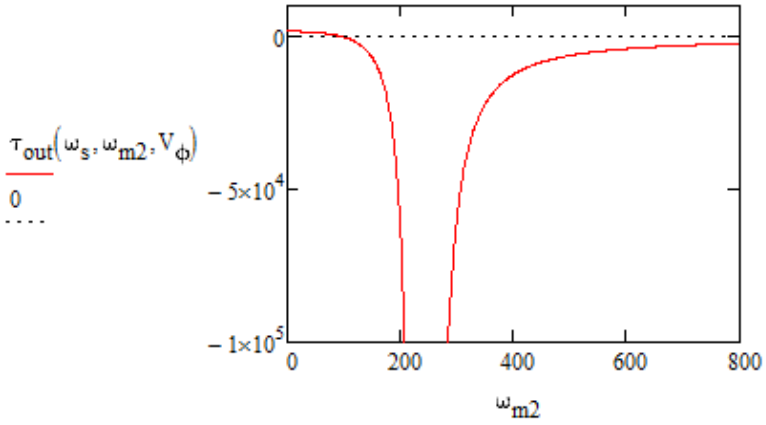

$$\frac{P(\omega_s, \omega_m, V_\phi)}{P_{in}(\omega_s, \omega_m, V_\phi)} = 88.394 \cdot \%$$

Appendix B

This appendix shows the development and calculation of the optimized model. The final model shows a machine of roughly 25 lbs and 88% efficiency.

Setting constant parameters

$V_1 := 35mph$

$d_1 := 9in$

$t_1 := 2in$

$D_1 := d_1 + 2t_1$ $\quad D_1 = 13 \cdot in$

Determining mechanical frequency

$f_m := \frac{V_1}{\pi \cdot D_1}$ $\quad f_m = 15.083 \cdot Hz$

Determining outside diameter of the stator based on number of poles

$D(P_1) := (d_1 - .5in) \cdot \frac{2 \cdot P_1}{2 \cdot P_1 + .01 \cdot \pi}$

Determining electrical frequency

$f_s(P_1) := P_1 \cdot f_m$

Desired power

$P_s := 25hp$

Number of phase belts per pole

$q := 3$

$L_1 := 4in$

Determining air gap

$g_1(P_1) := \frac{.01 \cdot \pi \cdot D(P_1)}{2 \cdot P_1}$

$s_{ts} := .5in$ desired size of stator slot and tooth

$n_s(P_1) := \text{floor}\left[\frac{\left[\frac{\pi \cdot (D(P_1) + g_1(P_1))}{s_{ts}}\right]}{2 \cdot q \cdot P_1}\right]$

Determining factors as discussed in chapter 3

$$p_s(P_1) := \frac{\text{floor}\left(n_s(P_1)\cdot q\cdot\frac{5}{6}\right)}{n_s(P_1)\cdot q}$$

$$K_{ps}(P_1) := \sin\left(\frac{p_s(P_1)\cdot\pi}{2}\right)$$

$$K_{ds}(P_1) := \frac{\sin\left(\frac{\pi}{2\cdot q}\right)}{n_s(P_1)\cdot\sin\left(\frac{\pi}{2\cdot n_s(P_1)\cdot q}\right)}$$

$Slots_s(P_1) := q\cdot P_1\cdot 2\cdot n_s(P_1)$ number of slots

$$\tau_s(P_1) := \frac{\pi\cdot(D(P_1) + g_1(P_1))}{Slots_s(P_1)}$$

$$\tau_{ps}(P_1) := n_s(P_1)\cdot q\cdot\tau_s(P_1)$$

$width_i := .04mm$ +

determining the number of slots based on pole pairs and wire size

$$num_s(P_1, AWG_s) := \text{floor}\left[\frac{\sqrt{2\cdot\left(\frac{D(P_1)}{2}+\frac{g_1(P_1)}{2}\right)^2\cdot\left(1-\cos\left(\frac{.54\cdot\tau_s(P_1)}{\frac{D(P_1)}{2}+\frac{g_1(P_1)}{2}}\right)\right)}}{wired_{AWG_s} + width_i}\right]$$

$$b_{os}(P_1, AWG_s) := \left(\frac{D(P_1)}{2}+\frac{g_1(P_1)}{2}\right)\cdot\text{acos}\left[1-\left[\frac{\left[num_s(P_1, AWG_s)\cdot\left(wired_{AWG_s} + width_i\right)\right]^2}{2\cdot\left(\frac{D(P_1)}{2}+\frac{g_1(P_1)}{2}\right)^2}\right]\right] + width_i$$

$$t_{os}(P_1, AWG_s) := \tau_s(P_1) - b_{os}(P_1, AWG_s)$$

$$k_{cs}(P_1, AWG_s) := \frac{\tau_s(P_1)}{\tau_s(P_1) - \frac{2\cdot b_{os}(P_1, AWG_s)}{\pi}\cdot\left[\text{atan}\left(\frac{b_{os}(P_1, AWG_s)}{2\cdot g_1(P_1)}\right) - \frac{g_1(P_1)}{b_{os}(P_1, AWG_s)}\cdot\ln\left[1+\left(\frac{b_{os}(P_1, AWG_s)}{2\cdot g_1(P_1)}\right)^2\right]\right]}$$

$$k_c(P_1, AWG_s) := k_{cs}(P_1, AWG_s)^2$$

Determining effective air gap

$$g_e(P_1, AWG_s) := k_c(P_1, AWG_s)\, g_1(P_1)$$

$$\chi_s(P_1, AWG_s) := \frac{b_{os}(P_1, AWG_s)}{\frac{D(P_1)}{2} + \frac{g_1(P_1)}{2}} \cdot P_1$$

$$K_{\chi s}(P_1, AWG_s) := \operatorname{sinc}\left(\frac{\chi_s(P_1, AWG_s)}{2}\right)$$

$$\sigma_s(P_1) := \frac{P_1 \cdot 2 \cdot \pi}{Slots_s(P_1)}$$

$$Skew_s := 0$$

$$\alpha_s(P_1) := Skew_s \cdot \sigma_s(P_1)$$

$$K_{ss}(P_1) := \operatorname{sinc}\left(\frac{\alpha_s(P_1)}{2}\right)$$

$$K_s(P_1, AWG_s) := K_{ps}(P_1) \cdot K_{ds}(P_1) \cdot K_{\chi s}(P_1, AWG_s) \cdot K_{ss}(P_1)$$

Determining resistances

$$\rho_{copper70} := 1.72 \cdot 10^{-8} \cdot \Omega \cdot m \cdot [1 + 0.00426 \cdot (70 - 20)]$$

$$\rho_{al70} := 2.65 \cdot 10^{-8} \cdot \Omega \cdot m \cdot [1 + 0.00426 \cdot (70 - 20)] \qquad \rho_{rotor} := \rho_{al70}$$

$$R_s(P_1, N_s, AWG_s) := \frac{\left[\sqrt{L_1^2 + \left(Skew_s \cdot \tau_s(P_1)\right)^2} + p_s(P_1) \cdot \tau_{ps}(P_1) + wired_{AWG_s}\right] \cdot 2 \cdot N_s \cdot \rho_{copper70}}{\pi \cdot \left(\frac{wired_{AWG_s}}{2}\right)^2}$$

$$R_r(P_1, N_s, AWG_s) := \frac{\rho_{rotor}}{\rho_{copper70}} \cdot R_s(P_1, N_s, AWG_s)$$

$$T_s(P_1, N_s) := \frac{3 \cdot N_s}{Slots_s(P_1)}$$

Determining slot parameters and effective turns

$$Depth_{sslot}(P_1, N_s, AWG_s) := \frac{2 \cdot T_s(P_1, N_s) \cdot \left(wired_{AWG_s} + width_i\right)}{num_s(P_1, AWG_s)} + width_i$$

$$N_{si}(P_1) := \frac{Slots_s(P_1)}{3 \cdot n_s(P_1)}$$

$$D_s(P_1) := D(P_1) - g_1(P_1)$$

$$D_i(P_1, N_s, AWG_s) := D_s(P_1) - 3 \cdot Depth_{sslot}(P_1, N_s, AWG_s)$$

$$\rho_{iron} := 0.298 \cdot \frac{lbf}{in^3} \qquad L_1 = 4 \cdot in$$

Estimating machine weight

$$weight_s(P_1, N_s, AWG_s) := \left[\left(\frac{D_s(P_1)}{2}\right)^2 - \left(\frac{D_i(P_1, N_s, AWG_s)}{2}\right)^2\right] \cdot \pi \cdot L_1 \cdot \rho_{iron}$$

Setting minimum and maximum voltages, step sizes, and optimization parameters

$V_{min} := 100V$ $V_{max} := 600V$ $V_{step} := 10V$ $z_1 := 4$

$PP_{min} := 1$ $PP_{max} := floor\left[\frac{(d_1 - .5in) \cdot \pi}{s_{ts} \cdot 1 \cdot q \cdot 2}\right]$ $PP_{max} = 8$ maximum number of pole pairs

$m_1 := 40$ $c_1 := .4$ $e_1 := 0.9$ efficiency set point

$W_{max} := 35 \cdot lbf$ max weight

Optimizing Design for weight and efficiency

$Design :=$ $Op \leftarrow 1 + z_1$

$E_{sf} \leftarrow 0$

$PP_f \leftarrow 0$

$AWG_{sf} \leftarrow 0$

$N_{sf} \leftarrow 0$

$E_s \leftarrow V_{min}$

while $E_s \le V_{max}$

$AWG_i \leftarrow AWG\left(\frac{P_s}{\sqrt{3} \cdot E_s}\right)$

$AWG_i \leftarrow 1 \text{ if } AWG_i < 1$

$PP \leftarrow PP_{max}$

while $PP \geq PP_{min}$

$AWG_s \leftarrow AWG_i$

while $\left(num_s(PP, AWG_s) > 0\right) \wedge AWG_s \geq 1$

$N_i \leftarrow N_{si}(PP)$

$N_s \leftarrow N_i$

while $N_s < m_1 \cdot N_i$

$x_1 \leftarrow 0$

$x_1 \leftarrow 1 \text{ if } D_i(PP, N_s, AWG_s) \leq 0$

$$\Phi_M \leftarrow \frac{E_s \cdot \sqrt{2}}{2 \cdot \pi \cdot f_s(PP) \cdot K_s(PP, AWG_s) \cdot N_s \cdot \sqrt{3}}$$

$$I_s \leftarrow \frac{\sqrt{2} \cdot PP^2 \cdot g_e(PP, AWG_s) \cdot \Phi_M \cdot \pi}{2 \cdot \mu_0 \cdot q \cdot N_s \cdot K_s(PP, AWG_s) \cdot D(PP) \cdot L_1}$$

$x_1 \leftarrow 1 \text{ if } I_s > wirea_{AWG_s}$

$x_1 \leftarrow 1 \text{ if } P_s \geq \sqrt{3} \cdot E_s \cdot I_s$

$W \leftarrow weight_s(PP, N_s, AWG_s)$

$P_L \leftarrow 3 \cdot \left(R_s(PP, N_s, AWG_s) + R_r(PP, N_s, AWG_s)\right) \cdot I_s^2$

$x_1 \leftarrow 1 \text{ if } W > W_{max}$

$x_1 \leftarrow 1 \text{ if } P_L > (1 - e_1) \cdot \sqrt{3} \cdot E_s \cdot I_s$

$$x_1 \leftarrow 1 \text{ if } Op > z_1 \cdot \frac{W_{max}}{W} + \frac{(1 - e_1) \cdot \sqrt{3} \cdot E_s \cdot I_s}{P_L}$$

$$Op \leftarrow z_1 \cdot \frac{35lbf}{W} + \frac{(1 - e_1) \cdot \sqrt{3} \cdot E_s \cdot I_s}{P_L} \text{ if } x_1 < 1$$

$E_{sf} \leftarrow E_s \text{ if } x_1 < 1$

$PP_f \leftarrow PP \text{ if } x_1 < 1$

$AWG_{sf} \leftarrow AWG_s \text{ if } x_1 < 1$

$N_{sf} \leftarrow N_s \text{ if } x_1 < 1$

$N_s \leftarrow N_s + N_i$

$AWG_s \leftarrow AWG_s - 1$

$PP \leftarrow PP - 1$

$E_s \leftarrow E_s + V_{step}$

$Design_0 \leftarrow \frac{E_{sf}}{V}$

$Design_1 \leftarrow PP_f$

$Design_2 \leftarrow AWG_{sf}$

$Design_3 \leftarrow N_{sf}$

return Design

Optimized design parameters

$E_s := Design_0 \cdot V \qquad E_s = 500\,V$

$P_1 := Design_1 \qquad P_1 = 4$

$AWG_s := Design_2 \qquad AWG_s = 12 \qquad f_e := f_s(P_1) = 60.332 \cdot Hz$

$N_s := Design_3 \qquad N_s = 168$

$$\Phi_M := \frac{E_s \cdot \sqrt{2}}{2 \cdot \pi \cdot f_s(P_1) \cdot K_s(P_1, AWG_s) \cdot N_s \cdot \sqrt{3}} \qquad \Phi_M = 6.886 \times 10^{-3}\,Wb$$

$$I_s := \frac{\sqrt{2} \cdot P_1^{\,2} \cdot g_e(P_1, AWG_s) \cdot \Phi_M \cdot \pi}{2 \cdot \mu_0 \cdot q \cdot N_s \cdot K_s(P_1, AWG_s) \cdot D(P_1) \cdot L_1} \qquad I_s = 30.089\,A$$

$wirea_{AWG_s} = 41\,A$

$P_s := \sqrt{3} \cdot E_s \cdot I_s \qquad P_s = 26.058 \cdot kW \qquad D_s := D_s(P_1) \qquad D_s = 8.434 \cdot in$

$P_L := 3 \cdot \left(R_s(P_1, N_s, AWG_s) + R_r(P_1, N_s, AWG_s)\right) \cdot I_s^{\,2} \qquad P_L = 2.549 \times 10^{3}\,W$

$weight_s := weight_s(P_1, N_s, AWG_s) \qquad weight_s = 24.574 \cdot lbf \qquad e_s := \frac{P_s - P_L}{P_s} = 90.218 \cdot \%$

Final rotor and stator resistances

$r_r := R_r(P_1, N_s, AWG_s)$ $r_r = 0.569\,\Omega$

$r_s := R_s(P_1, N_s, AWG_s)$ $r_s = 0.369\,\Omega$

$\frac{r_s}{4.264 \cdot \Omega} = 0.087$

determining terms for main leakage term

$d_5 := 0 \quad d_4 := 0 \quad d_3 := 0 \quad w_1 := t_{os}(P_1, AWG_s) \quad w_2 := w_1 \quad d_{11} := Depth_{sslot}(P_1, N_s, AWG_s)$

$$P_{s1} := \left(\frac{d_5}{w_1} + \frac{2 \cdot d_4}{w_1 + w_2} + \frac{d_3}{w_2}\right) + \frac{d_{11}}{3 \cdot w_2}$$

Calculating leakage and magnetizing inductances

$K_{s1} := K_s(P_1, AWG_s)$

$N_{se} := \frac{4}{\pi} \cdot K_{s1} \cdot N_s$ $N_{se} = 199.12$

$r := \frac{D(P_1)}{2}$ $g_2 := g_e(P_1, AWG_s)$ $g_2 = 1.584 \cdot mm$

$$L_{ls1} := \frac{4 \cdot q \cdot N_{se}^{\,2} \cdot L_1 \cdot P_{s1} \cdot 12.57 \cdot 10^{-9} \cdot \frac{H}{cm}}{Slots_s(P_1)} \qquad L_{ls1} = 0.793 \cdot mH$$

$$L_e := \frac{7}{2 \cdot \pi} \cdot \frac{q \cdot N_{se}^{\,2} \cdot D_s \cdot \frac{H}{m}}{(2 \cdot P_1)^2 \cdot 10^6} \cdot (p_s(P_1) - 0.3)$$

$$L_{ms} := \frac{3}{2} \cdot \left(\frac{N_{se}}{2 \cdot P_1}\right)^2 \cdot \mu_0 \cdot \pi \cdot \frac{r \cdot L_1}{g_2} \qquad L_{ms} = 25.309 \cdot mH$$

$$L_z := \frac{\pi^2}{12} \cdot \left[\frac{4 (P_1)^2}{Slots_s(P_1)^2}\right] \cdot L_{ms} = 0.578 \cdot mH \qquad D(P_1) = 8.467 \cdot in$$

$L_{ls12} := L_{ls1} + L_e + L_z$

$L_{ls} := L_{ls12} = 1.608 \cdot mH$ $\quad \frac{L_{ls}}{L_{ms}} = 6.353 \cdot \%$

Setting parameters for steady state model

$R_1 := r_s$ $\quad R_2 := r_r$ $\quad L_M := L_{ms}$ $\quad PP := P_1$

$L_{11} := L_{ls}$ $\quad L_2 := L_{11}$ $\quad j := \sqrt{-1}$

$V_{LL} := E_s$ $\quad f_{sys} := f_e$ $\quad V_\phi := \frac{V_{LL}}{\sqrt{3}}$ $\quad \omega_s := f_{sys} \cdot 2 \cdot \pi$ $\quad \omega_{sm} := \frac{\omega_s}{PP}$

$s_1(\omega_{sm}, \omega_m) := \frac{\omega_{sm} - \omega_m}{\omega_{sm}}$ $\quad \omega_s = 379.077 \frac{1}{s}$

Determining the eqivalent impedance

$$Z_{eq}(\omega_s, \omega_m) := j \cdot \omega_s \cdot L_{11} + R_1 + \left[\frac{1}{\left(\frac{1}{j \cdot \omega_s \cdot L_M} \right) + \left[\frac{1}{\left(\frac{R_2}{s_1\left(\frac{\omega_s}{PP}, \omega_m \right)} \right) + j \cdot \omega_s \cdot L_2} \right]} \right]$$

Determining line current

$$I_{line}(\omega_s, \omega_m, V_\phi) := \frac{V_\phi}{Z_{eq}(\omega_s, \omega_m)}$$

Determining input power

$$P_{in}(\omega_s, \omega_m, V_\phi) := Re\left(3 \cdot V_\phi \cdot \overline{I_{line}(\omega_s, \omega_m, V_\phi)}\right)$$

Determining rotor current

$$I_r(\omega_s, \omega_m, V_\phi) := \frac{j \cdot \omega_s \cdot L_M}{j \cdot \omega_s \cdot L_M + \frac{R_2}{s_1\left(\frac{\omega_s}{PP}, \omega_m \right)} + j \cdot \omega_s \cdot L_2} \cdot I_{line}(\omega_s, \omega_m, V_\phi)$$

Determining output power

$$P(\omega_s, \omega_m, V_\phi) := 3 \cdot \left(\left| I_r(\omega_s, \omega_m, V_\phi) \right| \right)^2 \cdot \frac{\left(1 - s_1\left(\frac{\omega_s}{PP}, \omega_m \right) \right)}{s_1\left(\frac{\omega_s}{PP}, \omega_m \right)} \cdot R_2$$

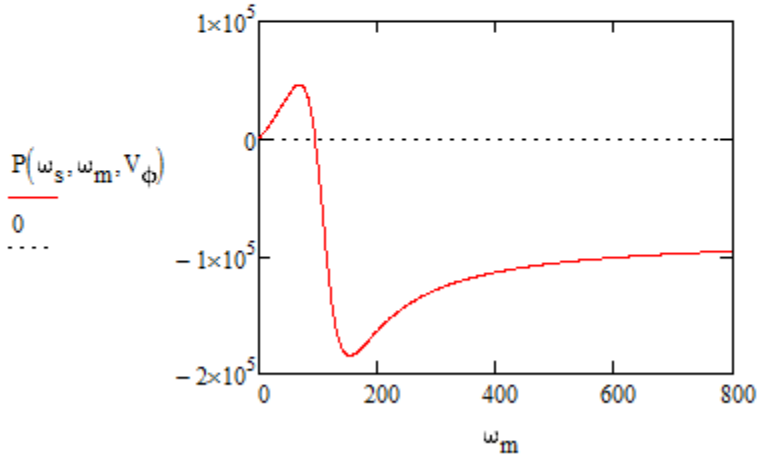

Determining Load torque

$$\tau_{out}(\omega_s, \omega_m, V_\phi) := \frac{P(\omega_s, \omega_m, V_\phi)}{\omega_m}$$

$$\omega_m := 88.2 \cdot \frac{rad}{s}$$

$$P(\omega_s, \omega_m, V_\phi) = 2.27 \times 10^4 \, W$$

Given

$$P(\omega_s, \omega_m, V_\phi) = 18kW$$

$$\omega_m := Find(\omega_m)$$

$$\omega_m = 89.787 \cdot \frac{rad}{s}$$

$$\omega_{sm} = 94.769 \cdot \frac{rad}{s}$$

$$\frac{\omega_{sm} - \omega_m}{\omega_{sm}} = 0.053$$

$$\tau_{out}(\omega_s, \omega_m, V_\phi) = 200.475 \cdot N \cdot m$$

$$\left| I_{line}(\omega_s, \omega_m, V_\phi) \right| = 37.504 \, A$$

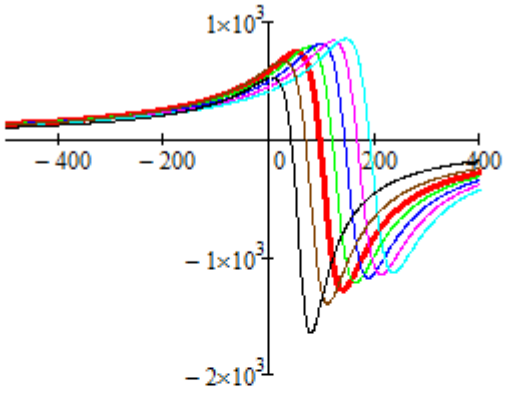

Design Point at 35 mph
40 mph operation
50 mph operation
60 mph operation
70 mph operation
25 mph operation
15 mph operation

$$\frac{P(\omega_s, \omega_m, V_\phi)}{P_{in}(\omega_s, \omega_m, V_\phi)} = 87.56 \cdot \%$$

efficiency at the design point

Appendix C

The following is the matlab script written to set the values for the simulink model. This script simply takes the values calculated in Appendix B and applies them to a dynamic model.

```
%% Jaz Veach
% Linear Induction Motor
% Parameter settings and calculations

%% clearing and setting the variables
close all

%% givens
rs =.369; % [ ohms] stator resistance
rpr = .569; % [ohms] rotor resistance referred to the primary
J1 = 36.12/4; % [ kg-m^2] inertia of the machine
Lm = 25.309e-3; % [H] magnetizing inductance
Lls = 1.207e-3; % [H] leakage on the stator
Lplr = Lls; % [H] leakage on the rotor referred to the primary
Vll = 500; % [V] line to line voltage of the system
Phs = 3; % number of phases of the system
wre = 3; % number of wires
Pe = 18.926; % [kW] machine power
Pole = 8; % number of poles
fe = 60.332;% [Hz] electrical frequency
B = 0; % friction
Tl = 200; %[Nm] load torque

%% calculating electrical frequency
w_e = 2*pi()*fe; % electrical frequency in rad/s

%% defining the reference frame
w = w_e; % stationary reference frame
```


```
%% defining the reference frame
w = w_e; % stationary reference frame
```


```
%% calculating VL
Vl = sqrt(2/3)*Vll; %% this calculates the amplitude of the voltage waveforms

%% calculations
a = exp(j*((2*pi()/3)));
```